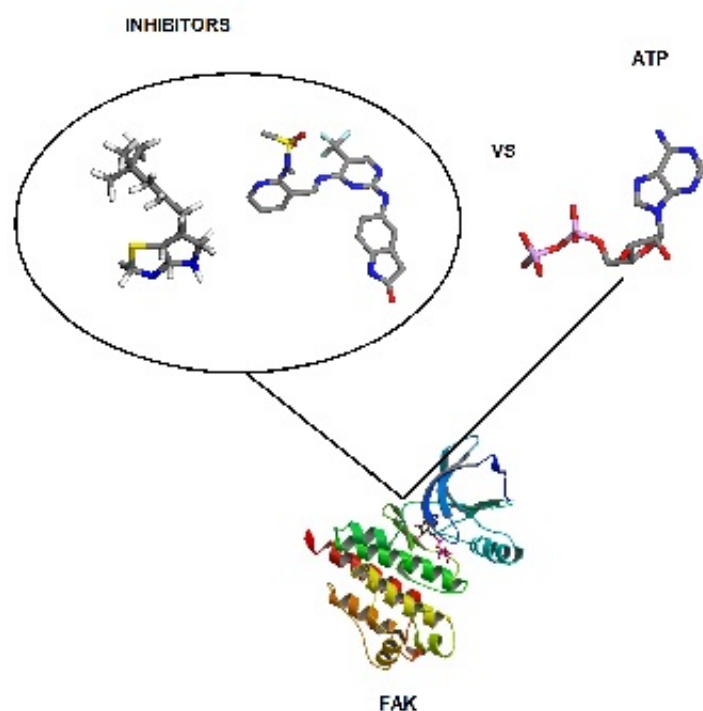


Eclética Química Journal

Volume 43 • number 3 • year 2018



**The correlation
between electronic
structure and
antitumor activity of a
selective focal
adhesion kinase
inhibitors**

Antioxidant

**Antioxidant capacity of
Melissa Officinalis L. on
Biological Systems**

Micropollutants

**Validation of analytical
methodology for determination of
Personal Care Products in
environmental matrix by GC-MSMS**

Geoprocessing

**Determination of the concentration
of Ce, La, Sm and Eu in a
phosphogypsum stack, in Imbituba
city, Santa Catarina, Brazil**

Rice husk

**Biosorption of 5G blue
reactive dye using
waste rice husk**

unesp 

UNIVERSIDADE ESTADUAL PAULISTA
"JÚLIO DE MESQUITA FILHO"

Instituto de Química
UNESP
Araraquara

ISSN 1678-4618



UNIVERSIDADE ESTADUAL PAULISTA

Reitor

Sandro Roberto Valentini

Vice-reitor

Sergio Roberto Nobre

Pró-reitor de Planejamento Estratégico e Gestão

Leonardo Theodoro Büll

Pró-reitora de Graduação

Gladis Massini-Cagliari

Pró-reitor de Pós-Graduação

João Lima Sant'Anna Neto

Pró-reitora de Extensão Universitária

Cleopatra da Silva Planeta

Pró-reitor de Pesquisa

Carlos Frederico de Oliveira Graeff



INSTITUTO DE QUÍMICA

Diretor

Eduardo Maffud Cilli

Vice-Diretora

Dulce Helena Siqueira Silva

Editorial Team

Editors

Prof. Assis Vicente Benedetti, Institute of Chemistry Unesp Araraquara, Brazil (Editor-in-Chief)

Prof. Arnaldo Alves Cardoso, Institute of Chemistry Unesp Araraquara, Brazil

Prof. Antonio Eduardo Mauro, Institute of Chemistry Unesp Araraquara, Brazil

Prof. Horacio Heinzen, Faculty of Chemistry, UdelaR, Montevideo, Uruguay

Prof. Maysa Furlan, Institute of Chemistry Unesp Araraquara, Brazil

Prof. Maria Célia Bertolini, Institute of Chemistry Unesp Araraquara, Brazil

Prof. Paulo Clairmont Feitosa de Lima Gomes, Institute of Chemistry, Unesp Araraquara, Brazil

Editorial Board

Prof. Jairton Dupont, Instituto de Química, Universidade Federal do Rio Grande do Sul, UFRGS, RS, Brazil

Prof. Enric Brillas, Facultat de Química, Universitat de Barcelona, Spain

Prof. Verónica Cortés de Zea Bermudez, Escola de Ciências da Vida e do Ambiente, Universidade de Trás-os-Montes e Alto Douro, Vila Real, Portugal

Prof. Lauro Kubota, Instituto de Química, Universidade Estadual de Campinas, Unicamp, SP, Brazil

Prof. Ivano Gerardt Rolf Gutz, Instituto de Química, Universidade de São Paulo, USP, SP, Brazil

Prof. Massuo Jorge Kato, Instituto de Química, Universidade de São Paulo, USP, SP, Brazil

Prof. Francisco de Assis Leone, Faculdade de Filosofia, Ciências e Letras, Universidade de São Paulo, Ribeirão Preto, USP-RP, SP, Brazil

Prof. Roberto Santana da Silva, Faculdade de Ciências Farmacêuticas, Universidade de São Paulo, Ribeirão Preto, USP-RP, SP, Brazil

Prof. José Antônio Maia Rodrigues, Faculdade de Ciências, Universidade do Porto, Portugal

Prof. Bayardo Baptista Torres, Instituto de Química, Universidade de São Paulo, USP, SP, Brazil

Technical Staff

Gustavo Marcelino de Souza
Lucas Henrique de Carvalho Machado

Editorial

The Editor is pleased to announce the third issue of **Eclética Química Journal** of 2018, which contains original articles covering different aspects of theoretical, analytical, environmental chemistry and physical-chemistry. In accordance with the scope of EQJ, the following subjects are being presented: the correlation between electronic structure and antitumor activity of a selective focal adhesion kinase (FAK) inhibitors, being the FAK responsible to phosphorylate other enzymes associated with signal transduction and it is found overexpressed in the organism during metastasis; evaluation *in vitro* antioxidant capacity of Melissa extract and its protective effect on peroxy radical-induced oxidative damage in erythrocytes; analytical methodology for quantifying personal care products, many of them with biological activity in the aquatic environment; determination of rare-earth elements in phosphogypsum stacks, being the phosphogypsum a by-product of phosphate fertilizer industry known as agricultural gypsum; removal of 5G blue reactive dye by means of biosorption using the rice husk residue as a biosorbent.

The Editor and his team wish to express their sincere thanks to the authors and reviewers for their outstanding collaboration.

Assis Vicente Benedetti
Editor-in-Chief of EQJ

Instructions for Authors

Preparation of manuscripts

- **Only manuscripts in English will be accepted.** British or American usage is acceptable but they should not be mixed.
- **The corresponding author should submit the manuscript online:**
<http://revista.iq.unesp.br/ojs/index.php/eclética/author>
- **Manuscripts must be sent in editable files as *.doc, *.docx or *.odt.** The text must be typed using font style Times New Roman and size 11. Space between lines should be 1.5 mm and paper size A4.
- **The manuscript should be organized in sections as follows:** Introduction, Experimental, Results and Discussion, Conclusions, and References. Sections titles must be written in bold and numbered sequentially; only the first letter should be in uppercase letter. Subsections should be written in normal and italic lowercase letters. For example: **1. Introduction;** *1.1 History;* **2. Experimental;** *2.1 Surface characterization;* *2.1.1 Morphological analysis*
- **The cover letter should include:** the authors' full names, e-mail addresses, ORCID code and affiliations, and remarks about the novelty and relevance of the work. The cover letter should also contain the suggestion of 3 (three) suitable reviewers (please, provide full name, affiliation, and e-mail).
- **The first page of the manuscript** should contain the title, abstract and keywords. *Please, do not give authors names and affiliation, and acknowledgements since a double-blind reviewer system is used. Acknowledgements should be added to the proof only.*
- **All contributions should include** an Abstract (200 words maximum), three to five Keywords and a Graphical Abstract (8 cm wide and 4 cm high) with an explicative text (2 lines maximum).
- **References should be numbered** sequentially in superscript throughout the text and compiled in brackets at the end of the manuscript as follows:

Journal:

[1] Adorno, A. T. V., Benedetti, A. V., Silva, R. A. G. da, Blanco, M., Influence of the Al content on the phase transformations in Cu-Al-Ag Alloys, *Eclética Quím.* 28 (1) (2003) 33-38. <https://doi.org/10.1590/S0100-46702003000100004>.

Book:

[2] Wendlandt, W. W., *Thermal Analysis*, Wiley-Interscience, New York, 3rd ed., 1986, ch1.

Chapter in a book:

[3] Ferreira, A. A. P., Uliana, C. V., Souza Castilho, M. de, Canaverolo Pesquero, N., Foguel, N. V., Pilon dos Santos, G., Fugivara, C. S., Benedetti, A. V., Yamanaka, H., Amperometric Biosensor for Diagnosis of Disease, In: *State of the Art in Biosensors - Environmental and Medical Applications*, Rincken, T., ed., InTech: Rijeka, Croatia, 2013, Ch. 12.

Material in process of publication:

[4] Valente Jr., M. A. G., Teixeira, D. A., Lima Azevedo, D., Feliciano, G. T., Benedetti, A. V., Fugivara, C. S., Caprylate Salts Based on Amines as Volatile Corrosion Inhibitors for Metallic Zinc: Theoretical and Experimental Studies, *Frontiers in Chemistry*. <https://doi.org/10.3389/fchem.2017.00032>.

- Figures, Schemes, and Tables should be numbered sequentially and presented at the end of the manuscript.
- Nomenclature, abbreviations, and symbols should follow IUPAC recommendations.
- Figures, schemes, and photos already published by the same or different authors in other publications may be reproduced in manuscripts of **Eclét. Quím. J.** only with permission from the editor house that holds the copyright.
- Graphical Abstract (GA) should be a high-resolution figure (900 dpi) summarizing the manuscript in an interesting way to catch the attention of the readers and accompanied by a short explicative text (2 lines maximum). GA must be submitted as *.jpg, *.jpeg or *.tif.
- **Communications** should cover relevant scientific results and are limited to 1,500 words or three pages of the Journal, not including the title, authors' names, figures, tables and references. However, Communications suggesting fragmentation of complete contributions are strongly discouraged by Editors.
- **Review articles** should present state-of-the-art overviews in a coherent and concise form covering the most relevant aspects of the topic that is being revised and indicate the likely future directions of the field. Therefore, before beginning the preparation of a Review manuscript, send a letter (1 page maximum) to the Editor with the subject of interest and the main topics that would be covered in Review manuscript. The Editor will communicate his decision in two weeks. Receiving this type of manuscript does not imply acceptance to be published in **Eclét. Quím. J.** It will be peer-reviewed.
- **Short reviews** should present an overview of the state-of-the-art in a specific topic within the scope of the Journal and limited to 5,000 words. Consider a table or image as corresponding to 100 words. Before beginning the preparation of a Short Review manuscript, send a letter (1 page maximum) to the Editor with the subject of interest and the main topics that would be covered in the Short Review manuscript.
- **Technical Notes:** descriptions of methods, techniques, equipment or accessories developed in the authors' laboratory, as long as they present chemical content of interest. They should follow the usual form of presentation, according to the peculiarities of each work. They should have a maximum of 15 pages, including figures, tables, diagrams, etc.
- **Articles in Education in Chemistry and chemistry-correlated areas:** research manuscript related to undergraduate teaching in Chemistry and innovative experiences in undergraduate and graduate education. They should have a maximum of 15 pages, including figures, tables, diagrams, and other elements.
- **Special issues** with complete articles dedicated to Symposia and Congresses can be published by **Eclét. Quím. J.** under the condition that a previous agreement with Editors is established. All the guides of the journal must be followed by the authors.
- **Eclét. Quím. J.** Ethical Guides and Publication Copyright:

Before beginning the submission process, please be sure that all ethical aspects mentioned below were followed. Violation of these ethical aspects may prevent authors from submitting and/or publishing articles in **Eclet. Quim. J.**

- The corresponding author is responsible for listing as authors only researchers who have really taken part in the work, and for informing them about the entire manuscript content and for obtaining their permission for submitting and publishing.
- Authors are responsible for carefully searching for all the scientific work relevant to their reasoning irrespective of whether they agree or not with the presented information.
- Authors are responsible for correctly citing and crediting all data used from works of researchers other than the ones who are authors of the manuscript that is being submitted to **Eclet. Quim. J.**
- Citations of Master's Degree Dissertations and PhD Theses are not accepted; instead, the publications resulting from them must be cited.
- Explicit permission of a non-author who has collaborated with personal communication or discussion to the manuscript being submitted to **Eclet. Quim. J.** must be obtained before being cited.
- Simultaneous submission of the same manuscript to more than one journal is considered an ethical deviation and is conflicted to the declaration has been done below by the authors.
- Plagiarism, self-plagiarism, and the suggestion of novelty when the material was already published are unaccepted by **Eclet. Quim. J.**
- The word-for-word reproduction of data or sentences as long as placed between quotation marks and correctly cited is not considered ethical deviation when indispensable for the discussion of a specific set of data or a hypothesis.
- Before reviewing a manuscript, the *turnitin* anti-plagiarism software will be used to detect any ethical deviation.
- The corresponding author transfers the copyright of the submitted manuscript and all its versions to **Eclet. Quim. J.**, after having the consent of all authors, which ceases if the manuscript is rejected or withdrawn during the review process.
- Before submitting manuscripts involving human beings, materials from human or animals, the authors need to confirm that the procedures established, respectively, by the institutional committee on human experimentation and Helsinki's declaration, and the recommendations of the animal care institutional committee were followed. Editors may request complementary information on ethical aspects.
- When a published manuscript in EQJ is also published in other Journal, it will be immediately withdrawn from EQJ and the authors informed of the Editor decision.
- **Manuscript Submission**

For the first evaluation: the manuscripts should be submitted in three files: the cover letter as mentioned above, the graphical abstract and the entire manuscript.

The entire manuscript should be submitted as *.doc, *.docx or *.odt files.

The Graphical Abstract (GA) 900 dpi resolution is mandatory for this Journal and should be submitted as *.jpg, *.jpeg or *.tif files as supplementary file.

The cover letter should contain the title of the manuscript, the authors' names and affiliations, and the relevant aspects of the manuscript (no more than 5 lines), and the suggestion of 3 (three) names of experts in the subject: complete name, affiliation, and e-mail).

• **Resubmission** (manuscripts "rejected in the present form" or subjected to "revision"): a letter with the responses to the comments/criticism and suggestions of reviewers/editors should

accompany the revised manuscript. All modifications made to the original manuscript must be highlighted.

• **Editor's requirements**

Authors who have a manuscript accepted in **Eclética Química Journal** may be invited to act as reviewers.

Only the authors are responsible for the correctness of all information, data and content of the manuscript submitted to **Eclética Química Journal**. Thus, the Editors and the Editorial Board cannot accept responsibility for the correctness of the material published in **Eclética Química Journal**.

• **Proofs**

After accepting the manuscript, **Eclét. Quim. J.** technical assistants will contact you regarding your manuscript page proofs to correct printing errors only, i.e., other corrections or content improvement are not permitted. The proofs shall be returned in 3 working days (72 h) via e-mail.

• **Authors Declaration**

The corresponding author declares, on behalf of the other authors, that the article being submitted is original and has been written by the stated authors who are all aware of its content and approve its submission. Declaration should also state that the article has not been published previously and is not under consideration for publication elsewhere, that no conflict of interest exists and if accepted, the article will not be published elsewhere in the same form, in any language, without the written consent of the publisher.

• **Appeal**

Authors may only appeal once about the decision regarding a manuscript. To appeal against the Editorial decision on your manuscript, the corresponding author can send a rebuttal letter to the editor, including a detailed response to any comments made by the reviewers/editor. The editor will consider the rebuttal letter, and if deemed appropriate, the manuscript will be sent to a new reviewer. The Editor decision is final.

• **Contact**

Gustavo Marcelino de Souza (eletica@journal.iq.unesp.br)

Copyright Notice

The corresponding author transfers the copyright of the submitted manuscript and all its versions to Eclét. Quim. J., after having the consent of all authors, which ceases if the manuscript is rejected or withdrawn during the review process.

The articles published by **Eclética Química Journal** are licensed under the Creative Commons Attribution 4.0 International License.

SUMMARY

EDITORIAL BOARD.....	3
EDITORIAL.....	4
INSTRUCTIONS FOR AUTHORS.....	5

ORIGINAL ARTICLES

The correlation between electronic structure and antitumor activity of a selective focal adhesion kinase inhibitors.....	10
<i>Daniel Augusto Barra de Oliveira</i>	
Antioxidant capacity of <i>Melissa Officinalis</i> L. on Biological Systems.....	19
<i>Juliana Metzner Franco, Silvana Marina Piccoli Pugine, Antônio Márcio Scatoline, Mariza Pires de Melo</i>	
Validation of analytical methodology for determination of Personal Care Products in environmental matrix by GC-MSMS.....	30
<i>Tais Cristina Filipe, Franciane de Almeida Brehm Goulart, Alinne Mizukawa, Júlio César Rodrigues de Azevedo</i>	
Determination of the concentration of Ce, La, Sm and Eu in a phosphogypsum stack, in Imbituba city, Santa Catarina, Brazil.....	37
<i>Renata Coura Borges, Letícia Mombrini Marques, Cláudio Fernando Mahler, Alfredo Victor Bellido Bernedo</i>	
Biosorption of 5G blue reactive dye using waste rice husk.....	45
<i>Ismael Laurindo Costa Junior, Leandro Finger, Poliana Paula Quitaiski, Samuel Mathias Neitzke, Josue Victor Besen, Maike Krug Correa, Juliana Bortoli Rodrigues Mees</i>	

The correlation between electronic structure and antitumor activity of a selective focal adhesion kinase inhibitors

Daniel Augusto Barra de Oliveira¹ 

¹ University Federal of Tocantins, 34 Dois St, Araguaína, Tocantins, Brazil

* Corresponding author: Daniel Augusto Barra de Oliveira, phone: +55 63 99200-7791, e-mail address: danielchem@uft.edu.br

ARTICLE INFO

Article history:

Received: December 13, 2017

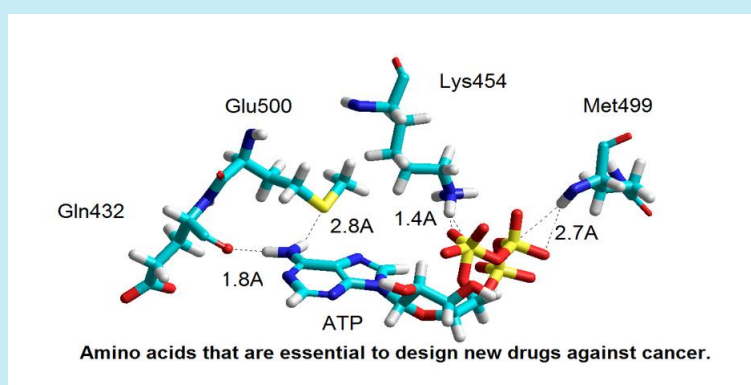
Accepted: September 25, 2018

Published: October 7, 2018

Keywords:

1. QM/MM
2. focal adhesion kinase
3. molecular docking
4. geometry optimization

ABSTRACT: Focal Adhesion Kinase (FAK) is a non-tyrosine kinase responsible to phosphorylate other enzymes associated with signal transduction. This biochemical process plays an important role to control cancer. FAK is found overexpressed in the organism during metastasis. Since FAK may be involved in the invasion and metastasis of cancer, novel molecules based on drug design have been synthesized over the past few years. The inhibitors are designed to mimic the natural substrate which is the ATP molecule. This work studied the hydrogen bonds performed between inhibitors and FAK and other electronic properties involved in this interaction. The molecular structure of FAK docked with the inhibitors was simulated using classical molecular dynamics. FAK/ inhibitor complex



obtained by dynamic was optimized using quantum mechanical *ab-initio* calculation. Our results show that all inhibitors interact with Cys502 located in the FAK-binding site. *Ab-initio* calculations show that HOMO orbital is situated under Met499 and Glu500 amino acids indicating chemical reactivity in this region. The results of molecular dynamics combined with quantum chemical calculations show that the sulfonamide has a strong hydrogen bond with close distances, while the thiazole has a weak hydrogen bond with long distances. Sulfonamide has known good activity against FAK while the thiazole molecule has an unknown activity. These results allow predicting that the molecule of thiazole is a not good inhibitor to FAK inhibition.

1. Introduction

Cancer is a disease whose feature is the uncontrolled proliferation of cells, able to spread to other tissues. Cell proliferation is related with the biochemical process known as signal transduction. FAK and other kinases are enzymes which catalyze these reactions. During the signal transduction mechanism, chemical signals provided from cell exteriors are converted into physical responses within the cells¹⁻⁷.

Focal adhesion kinase (FAK) is a non-tyrosine kinase involved in signal transduction, which is the

chemical process associated with the development of several kinds of cancers⁸⁻¹⁴. Consequently, the study of this enzyme is essential to design and synthesize new drugs against cancer. FAK acts in signal transduction mechanism promoting the phosphorylation of serine and tyrosine amino acids. Therefore, new drugs have been designed and synthesized to inhibit the phosphorylation of FAK. The basic chemical structure of these inhibitors is the adenine ring that mimics the ATP molecule.

The interactions among the amino acids in the FAK-binding site with different inhibitors have the

same pattern of hydrogen bonds, even in the case of quite different chemical structure of inhibitors^{15,16}. These chemical changes in the structure allow the drugs have different biological responses against the cancer. Pyrrolopyrimidine inhibitor has been synthesized in order to interact with Arg426, Cys502 and Lys545 in FAK binding site¹⁷.

The PDB ID 3BZ3 ligand (C₂₁ H₂₀ F₃ N₇ O₃ S)¹⁶ and ID PDB 3PXX ligand (C₁₂ H₁₄ N₂ S)¹⁵ are examples of molecules that have different molecular structures and different ways to inhibit FAK phosphorylation. PDB ID 3BZ3 ligand is a potent ATP inhibitor that shows inhibition against FAK in the cellular environment. This molecule is an ATP-competitive, reversible inhibitor of FAK and Pyk2 catalytic activity with an IC₅₀ of 1.5 and 14 nmol L⁻¹, respectively. Antitumor efficacy and regressions were observed in multiple human xenograft models for PDB ID 3BZ3 ligand. This drug has applications on the colon and lung cancer while the ID PDB 3PXX ligand (C₁₂ H₁₄ N₂ S) can induce apoptosis in different tumor lines. The differences of biological activity are linked to the molecular structure of inhibitors docked in the binding site.

Theoretical calculations permit to explore the interactions among the amino acids in the FAK-binding site with different inhibitors. Dynamical calculation can show the possible hydrogen bonds performed by the inhibitors while quantum mechanical calculation can describe important electronic properties. In this work, we described the pattern of hydrogen bonds at the catalytic site using molecular dynamics and quantum mechanical calculations in order to understand how these hydrogen bonds are linked to the FAK inhibition.

2. Materials and methods

2.1 Quantum Chemical and Molecular Dynamic Calculations

X-Ray molecular structure based on PDB ID 3BZ3¹⁶, 3PXX¹⁵, and 2IJM¹⁸ were used as initial geometry to describe the interaction of the methane sulfonamide diaminopyrimidine, pyrrolo[2,3-d]thiazole and ATP respectively. One nanosecond of molecular dynamics was performed to search possible hydrogen bonds. This simulation was calculated using the program Hyperchem¹⁹. An implicit solvent with dielectric constant equal to 80 was used in order to simulate the water solvent. The

constant temperature of 300 K was used during the simulation and NVE ensemble was used. Molecular optimization with the force field Charm²⁰ was performed in order to avoid atom superimposition before the molecular dynamics using a *steepest decent* algorithm. SwissParam²¹ was used to provide parameters and topologies for the ligands. Pair correlation function was calculated to hydrogen bonds inside the catalytic site. CHELPG charge derivative of HF/6-31G was used to describe atomic charge for the inhibitor inside the catalytic site for dynamic calculation. Molecular dynamic was used to search different hydrogen bonds. Quantum chemical calculations were used to describe the hydrogen bonds present in the FAK inhibitors interaction. The ONIOM²²⁻²⁵ method, present in a Gaussian program, was used to describe the molecular structures cited above. In order to depict the higher layer, the amino acids Cys502, Lys454, Met499, Arg426, Ala452, Glu506, Glu471, Arg508, Arg550, Asp564, Leu501, Glu430 and Thr605¹⁷ were selected from molecular dynamic results. The quantum mechanical calculations based on PM6, B3LYP/6-31g, HF/6-31g, RMNDO were employed in the higher layer that was optimized using the keyword *quadmac*²⁵. This keyword does a quadratic step in the coordinates of all the atoms. UFF (Universal Force Field) was used in order to describe the Vander Walls and electrostatic potential for the atoms in the lower layer. *Qeq*²⁶ method was used to get the charges for UFF²⁷ force field. Molecular frontier orbitals were calculated using HF *ab-initio* method. The hydrogen bond energies were investigated with electronic calculation MP2 and the base function 6-31G ++ (d, p) coupled to the CPCM method for water solvent. The strength of the hydrogen bonds was investigated using the interaction energy between the inhibitors and the amino acid.

3. Results and discussion

3.1 Quantum optimizations

HF 6-31G was the method used to describe the hydrogen bonds and other interactions for all inhibitors, because other methods did not perform a full convergence of biological systems studied. Successive errors associated with internal coordinates and the dihedral angles were observed for the methods PM6 and B3LYP/6-31g. MNDO semi-empirical method performed a full optimization for the entire biological system, but it

is a less robust approach when compared with HF approach. Therefore, the combination HF 6-31G and UFF were used to obtain the equilibrium geometry of the system FAK docked with all the inhibitors. The hydrogen bonds in the binding site obtained from ONIOM calculations are shown in [Figure 1](#).

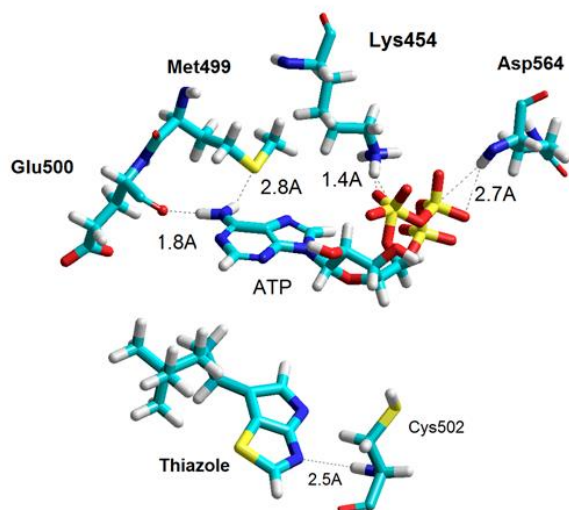


Figure 1. Hydrogen bonds performed by the inhibitors and the ATP molecule after ONIOM optimization.

The hydrogen bonds formed are similar to all inhibitors. Sulfonamide and the thiazole molecule perform hydrogen bonds with the amino acid Cys502. The thiazole molecule has a single interaction with the Cys502 amine group with 2.5 Å of distance. Sulfonamide performs two hydrogen bonds with Cys502 amino group with 2.3 Å and

other bond with hydroxyl group at 1.9 Å of distance. The Cys502 hydrogen bond has been seen on others FAK inhibitors in accord to literature¹⁷. Amber force field optimization for 7-h-pyrrolopyrimidine shows a hydrogen bond with a Cys502 amino group with 2.15 Å of distance. Quantum mechanical calculation did not show this hydrogen bond to the ATP molecule. Sulfonamide drug can interact yet with the Arg426 amino group with a distance of 1.9 Å. This hydrogen bond is found in 7-h-pyrrolopyrimidine inhibitors. The hydrogen bond with Asp424 is found in the 7-h-pyrrolopyrimidine inhibitor 32, which has the best IC_{50} between pyrrolopyrimidine drugs¹⁷.

ATP is a special case. There are hydrogen bonds with Gln432 and Glu500 that happen with the adenine ring. On the other hand, phosphate groups interact with the amino acids Lys454 and Met499. In recent literature¹⁷, the interaction with Lys454 has been associated with the increase of FAK inhibition. The most powerful pyrrolopyrimidine inhibitor, named 32, also interacts with the amino acid Met499¹⁷.

3.2 Molecular dynamics

The results of molecular dynamics and the pair correlation function are shown in the [Figure 2](#). The pair correlation function is related to the probability of finding the center of a particle a given distance from the center of another particle. [Figure 2](#) shows the probability of finding two atoms with a given separation.

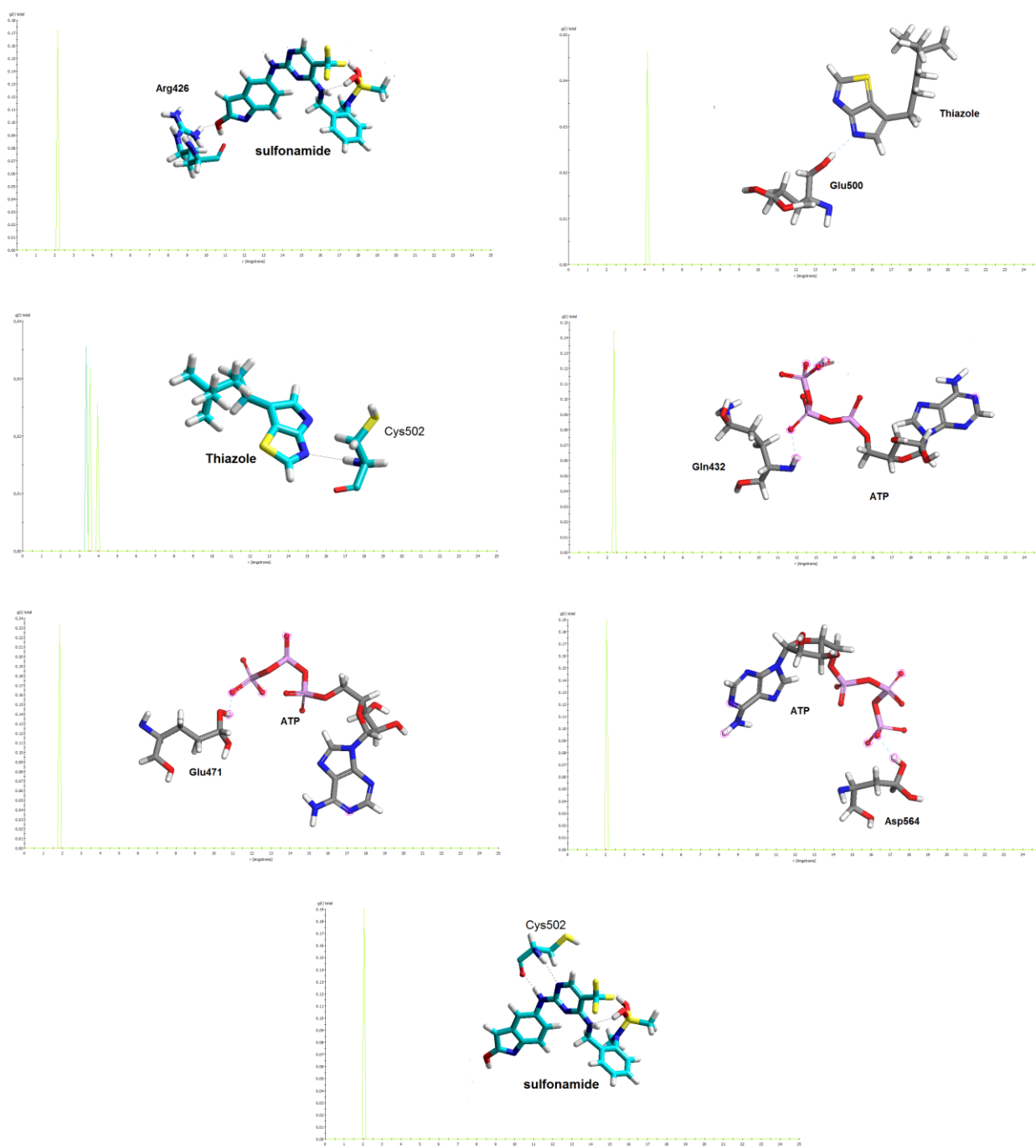


Figure 2. Hydrogen bonds performed by the inhibitors and ATP using molecular dynamics and the graphic of pair function correlation.

Molecular dynamic shows that the sulfonamide molecule can bind with Cys502 and Arg426. The average of binding distances is equal to 2 Å for both amino acids. Thiazole molecule performs a hydrogen bond with the amino acid Cys502 and the amino acid Glu500. An average of 4.0 Å of distance for these interactions was described by molecular dynamic calculation. ATP molecule

performs hydrogen bonds with Asp564, Gln432 and Glu471. The interaction with Gln432 and Asp564 is close to 2.5 Å while the interaction with Glu471 is close to 2.0 Å. These results show a distribution of hydrogen bond distances during the molecular dynamics. The differences between ONIOM (HF/6-31G/UFF) results compared with molecular dynamics are described in [Table 1](#).

Table 1. Hydrogen Bonds distances performed between the amino acids localized in the binding site and the inhibitors using different methodologies (MD- Molecular Dynamics and ONIOM, HF/6-31G/UFF).

<i>Amino acid</i>	<i>Sulfonamide ONIOM Hydrogen Bond Distances (Å)</i>	<i>Sulfonamide MD Hydrogen Bond Distances (Å)</i>	<i>Thiazole ONIOM Hydrogen Bond Distances (Å)</i>	<i>Thiazole MD Hydrogen Bond Distances (Å)</i>	<i>ATP ONIOM Hydrogen Bond Distances (Å)</i>	<i>ATP MD Hydrogen Bond Distances (Å)</i>
Lys454					1.4	1.6
Cys502	1.9, 2.3	****	2.5	4.0		2.5
Arg426	1.9	****				
Glu500				3.5-4.0	2.8	2.06
Met499					2.7	1.6
Gln432					1.8	2.5
Asp564	2.4	****				2.0

****No changes verified in the hydrogen bond distances compared with ONIOM optimization

The results of molecular dynamics are close to ONIOM approach. Sulfonamide molecule performs hydrogen bonds close to 2.0 Å for both methods. ATP molecule shows similar distances of hydrogen bond for the two methods. The exception is the molecule of Thiazole. During the molecular dynamic the hydrogen bond with Cys502 keep a distance close to 4.0 Å, while the ONIOM optimization shows a distance of 2.5 Å. The MP2 method shows that this bond has energy close to 1 kcal, while the same bond to sulfonamide has an energy interaction close to 40 kcal. The same result is seen to the interaction with Glu500. The energy to the interaction between the thiazole inhibitor and the amino acid Glu500 is close to 2 kcal. These

results justify the discrepancy between the quantum mechanical optimization and the molecular dynamics. There is no experimental quantity activity to thiazole molecule. However, we believe that this inhibitor does not have a good activity to FAK inhibition due to weak interaction energy with the FAK binding site associate with long hydrogen bond distances. On the other hand, the sulfonamide molecule has a good activity to inhibit FAK and very strong hydrogen bonds.

3.3 Orbitals analysis

The molecular orbitals obtained from *ab-initio* calculation are shown below in [Figure 3](#).

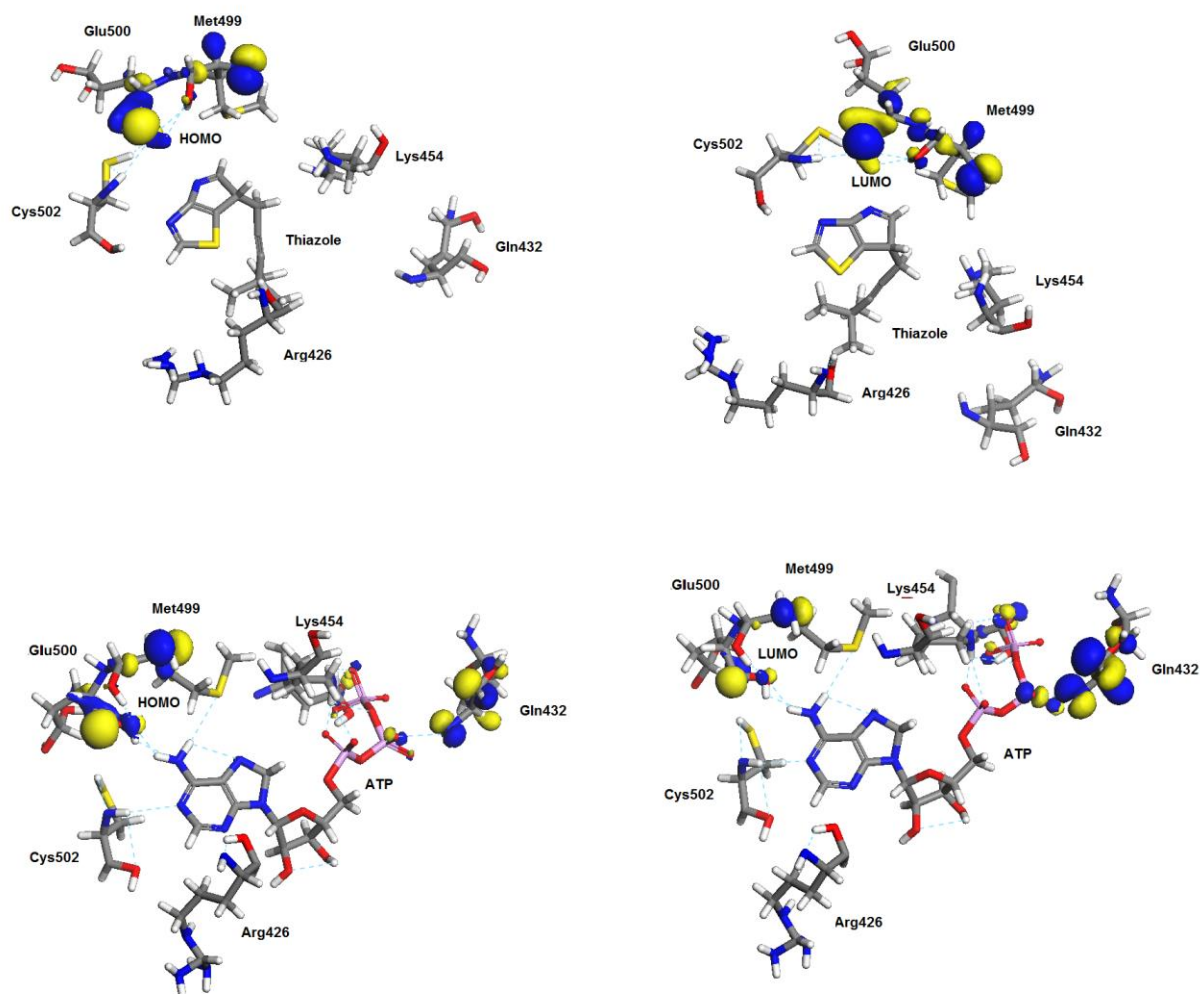


Figure 3. Molecular Orbitals HOMO and LUMO obtained from *ab-initio* calculations of the ligands (ATP, Sulfonamide and Thiazole) in the binding site.

The HOMO and LUMO molecular orbitals obtained from *ab-initio* calculations show a pattern in the binding site for the ligands studied. HOMO orbitals are located mainly in the amino acids Glu500 and Met499. In the ATP molecule, the LUMO orbital is located at the amino acid Gln432 while in the thiazole molecule, LUMO orbital remains on the amino acids Glu500 and Met499. The orbital of the sulfonamide is located on the amino acid Cys502. Fluorine atoms of the sulfonamide inhibitor interact with amino acids Met499 and Glu500, while in the ATP molecule the interaction occurs with the chemical group Adenine. The bicyclic ring of the thiazole molecule has the same function as the adenine ring of the

ATP molecule and the fluorine atoms of the sulfonamide molecule.

The construction of new inhibitors should be focused on towards the compliance of the hydrogen bonds obtained, as well as the arrangement of the HOMO / LUMO orbitals that emphasize the importance of the connections and interactions with the amino acids Met499 and Glu500. The inhibitor thiazole has a long hydrogen bond and a weak hydrogen bond with the amino acids where are localized the orbitals HOMO and LUMO. On the other hand, the inhibitor sulfonamide is close to HOMO and LUMO orbital at the same time and it has high bond energy. The sulfonamide has a low IC_{50} indicating that less quantity of molecule is necessary to inhibit FAK. The thiazole has

unknown quantity experimental data (IC_{50}). These data can reveal that thiazole can be not a good inhibitor to FAK.

4. Conclusions

We studied two inhibitors using two kinds of calculations (Molecular Dynamic and ONIOM quantum mechanical approach). Both calculations show similar hydrogen bonds to the inhibitors compared with ATP molecule. However, the hydrogen bond distances and the bond energies are different to inhibitors. Sulfonamide has a strong hydrogen bond with the amino acids Glu500 and Cys502 while the thiazole inhibitor has a weak hydrogen bond with these amino acids. Molecular dynamics show close hydrogen bonds to sulfonamide and long hydrogen bond distances to thiazole. HOMO orbital is localized close to amino acid Glu500 in the binding site. ATP and Sulfonamide are close to this orbital while the thiazole is far from the HOMO orbital. There is no number of activity (IC_{50}) to thiazole. However, these results show that thiazole molecule could have a low experimental activity against FAK, because the sulfonamide inhibitor has high activity with close hydrogen bonds to the amino acids (including the amino acids where are located HOMO and LUMO orbitals) of the catalytic site at the same time it has strong hydrogen bonds with these amino acids.

5. Acknowledgments

I am grateful for the technological support of LQC (Laboratory of Computational Chemistry-UnB).

6. References

- [1] McCubrey, J. A., Abrams, S. L., Stadelman, K., Chappell, W. H., LaHair, M., Ferland, R. A., Steelman, L. S., Targeting signal transduction pathways to eliminate chemotherapeutic drug resistance and cancer stem cells, *Adv. Enzyme Regu.* 50 (2010) 285-307. <https://doi.org/10.1016/j.advenzreg.2009.10.016>.
- [2] Collins, I., Workman, P., Design and development of signal transduction inhibitors for cancer treatment: Experience and challenges with kinase targets, *Current Signal Transduction Therapy* 1 (1) (2006) 13-23. <https://doi.org/10.2174/157436206775269181>.
- [3] Fulda, S., Debatin, K.-M., Signal transduction therapy targeting apoptosis pathways in cancers, *Current Signal Transduction Therapy* 1 (2) (2006) 179-190. <https://doi.org/10.2174/157436206777012075>.
- [4] Klein, S., Levitzki, A., Signal transduction therapy for cancer - Whither now? *Current Signal Transduction Therapy* 1 (1) (2006) 1-12. <https://doi.org/10.2174/157436206775269244>.
- [5] Christoffersen, T., Guren, T. K., Spindler, K.-L. G., Dahl, O., Lonning, P. E., Gjertsen, B. T., Cancer therapy targeted at cellular signal transduction mechanisms: Strategies, clinical results, and unresolved issues, *European Journal of Pharmacology* 625 (2009) 6-22. <https://doi.org/10.1016/j.ejphar.2009.10.009>.
- [6] Bidwell, G. L. III, Raucher, D., Therapeutic peptides for cancer therapy. Part I - peptide inhibitors of signal transduction cascades, *Expert Opinion on Drug Delivery* 6 (10) (2009) 1033-1047. <https://doi.org/10.1517/17425240903143745>.
- [7] Levitzki, A., Klein, S., Signal transduction therapy of cancer, *Molecular Aspects of Medicine* 31 (4) (2010) 287-329. <https://doi.org/10.1016/j.mam.2010.04.001>.
- [8] Huang, S.-M., Hsu, P.-C., Chen, M.-Y., Li, W.-S., More, S. V., Lu, K.-T., Wang, Y.-C., The novel indole compound SK228 induces apoptosis and FAK/Paxillin disruption in tumor cell lines and inhibits growth of tumor graft in the nude mouse, *International Journal of Cancer* 131 (2012) 722-732. <https://doi.org/10.1002/ijc.26401>.
- [9] Chang, S. K., Hinds, A., Cornelius, L. A., Efimova, T., Proline-rich tyrosine kinase 2 (Pyk2), a focal adhesion kinase (FAK) homologue, induces apoptosis in human malignant metastatic melanoma, *Journal of Investigative Dermatology* 132 (2012) 130-130. <https://doi.org/10.2353/ajpath.2008.080292>.
- [10] Kwak, S. W., Park, E. S., Lee, C. S., Parthenolide induces apoptosis by activating the mitochondrial and death receptor pathways and

inhibits FAK-mediated cell invasion, *Molecular and Cellular Biochemistry* 385 (2014) 133-144. <https://doi.org/10.1007/s11010-013-1822-4>.

[11] Shieh, J.-M., Wei, T.-T., Tang, Y.-A., Huang, S.-M., Wen, W.-L., Chen, M.-Y., Cheng, H.-C., Salunke, S. B., Chen, C.-S., Lin, P., Chen, C.-T., Wang, Y.-C., Mitochondrial Apoptosis and FAK Signaling Disruption by a Novel Histone Deacetylase Inhibitor, HTPB, in Antitumor and Antimetastatic Mouse Models, *Plos One* 7 (1) (2012) e30240. <https://doi.org/10.1371/journal.pone.0030240>.

[12] Yoon, H., Choi, Y.-L., Song, J.-Y., Do, I., Kang, S. Y., Ko, Y.-H., Song, S., Kim, B.-G., Targeted Inhibition of FAK, PYK2 and BCL-XL Synergistically Enhances Apoptosis in Ovarian Clear Cell Carcinoma Cell Lines, *Plos One* 9 (2) (2014) e88587. <https://doi.org/10.1371/journal.pone.0088587>.

[13] Vanamala, J., Radhakrishnan, S., Reddivari, L., Bhat, V. B., Ptitsyn, A., Resveratrol suppresses human colon cancer cell proliferation and induces apoptosis via targeting the pentose phosphate and the talin-FAK signaling pathways-A proteomic approach, *Proteome Science* 9 (1) (2011) 49. <https://doi.org/10.1186/1477-5956-9-49>.

[14] Kanteti, R., Mirzapoiyazova, T., Riehm, J. J., Dhanasingh, I., Mambetsariev, B., Wang, J., Kulkarni, P., Kaushik, G., Seshacharyulu, P., Ponnusamy, M. P., Kindler, H. L., Nasser, M. W., Batra, S. K., Salgia, R., Focal adhesion kinase a potential therapeutic target for pancreatic cancer and malignant pleural mesothelioma, *Cancer Biology Therapy* 19 (4) (2018) 316-327. <https://doi.org/10.1080/15384047.2017.1416937>.

[15] Roberts, W. G., Ung, E., Whalen, P., Cooper, B., Hulford, C., Autry, C., Richter, D., Emerson, E., Lin, J., Kath, J., Coleman, K., Yao, L., Martinez-Alsina, L., Lorenzen, M., Berliner, M., Luzzio, M., Patel, N., Schmitt, E., LaGreca, S., Jani, J., Wessel, M., Marr, E., Griffor, M., Vajdos, F., Antitumor activity and pharmacology of a selective focal adhesion kinase inhibitor, PF-562,271, *Cancer R.* 15 (2008) 1935-1944. <https://doi.org/10.1158/0008-5472.CAN-07-5155>.

[16] Koolman, H., Heinrich, T., Musil, D., Co-crystal Structures of FAK with an Unprecedented

Pyrrolo[2,3-d]thiazole, Accessed in June 2017 <https://www.rcsb.org/structure/3pxk>.

[17] Barra de Oliveira, D. A., de Oliveira Neto, M., Martins, J. B. L., Theoretical study of disubstituted pyrrolopyrimidines as focal adhesion kinase inhibitors, *International Journal of Quantum Chemistry* 10 (2012) 2324-2329. <https://doi.org/10.1002/qua.23181>.

[18] Andersen, C. B., Ng, K., Ficarro, S., Vu, C., Choi, H.-S., He, Y., Spraggon, G., Gray, N., Lee, C. C., Crystal Structure of Focal Adhesion Kinase Catalytic Domain Complexed with ATP and Novel 7H-Pyrrolo [2,3-d] pyrimidine Inhibitor Scaffolds, Accessed in June 2017. <https://www.rcsb.org/structure/2ijm>.

[19] HyperChem(TM) Professional 7.51, Hypercube, Inc., 1115 NW 4th Street, Gainesville, Florida 32601, USA.

[20] Brooks, B. R., Bruccoleri, R. E., Olafson, B. D., States, D. J., Swaminathan, S., Karplus, M. "CHARMM: A program for macromolecular energy, minimization, and dynamics calculations", *J. Comp. Chem.* 4 (2) (1983) 187-217. <https://doi.org/10.1002/jcc.540040211>.

[21] Zoete, V., Cuendet, M. A., Grosdidier, A., Michielin, O., SwissParam: A Fast Force Field Generation Tool For Small Organic Molecules, *J. Comput. Chem.* 32 (11) (2011) 2359-68. PMID: 21541964. <https://doi.org/10.1002/jcc.21816>.

[22] Dapprich, S., Komáromi, I., Byun, K. S., Morokuma, K., Frisch, M. J., A New ONIOM Implementation in Gaussian 98. Part 1. The Calculation of Energies, Gradients and Vibrational Frequencies and Electric Field Derivatives, *J. Mol. Struct. (Theochem)* 462 (1999) 1-21. [https://doi.org/10.1016/S0166-1280\(98\)00475-8](https://doi.org/10.1016/S0166-1280(98)00475-8).

[23] Vreven T., Morokuma, K., Hybrid Methods: ONIOM(QM:MM) and QM/MM, *Annual Reports in Comp. Chem.* 2 (2006) 35-51. [https://doi.org/10.1016/S1574-1400\(06\)02003-2](https://doi.org/10.1016/S1574-1400(06)02003-2).

[24] Vreven, T., Byun, K. S., Komaromi, I., Dapprich, S., Montgomery Jr., J.A., Morokuma, K., Frisch, M. J., Combining Quantum Mechanics Methods with Molecular Mechanics Methods in ONIOM, *J. of Chem. Theory and Computation* 2

(3) (2006) 815-826.
<https://doi.org/10.1021/ct050289g>.

[25] Vreven, T., Frisch, M. J., Kudin, K. N., Schlegel, H. B., Morokuma, K., Geometry optimization with QM/MM Methods. II. Explicit Quadratic Coupling, *Mol. Phys.*, 104 (2006) 701-714. <https://doi.org/10.1080/00268970500417846>.

[26] Rappé, A. K., Goddard III, W. A., "Charge equilibration for molecular-dynamics simulations," *J. Phys. Chem.* 95 (1991) 3358-3363. <https://doi.org/10.1021/j100161a070>.

[27] Rappé, A. K., Casewit, C. J., Colwell, K. S., Goddard III, W. A., Skiff, W. M., UFF, a Full Periodic Table Force Field for Molecular Mechanics and Molecular Dynamics Simulations, *J. Am. Chem. Soc.* 114 (1992) 10024–10035. [0002-786319211514-10024%03.00/0](https://doi.org/10.1021/cr00027a002).

Antioxidant capacity of *Melissa Officinalis* L. on Biological Systems

Juliana Metzner Franco¹, Silvana Marina Piccoli Pugine¹, Antônio Márcio Scatoline¹, Mariza Pires de Melo¹

¹ Faculty of Animal Science and Food Engineering (FZEA), University of São Paulo, Pirassununga, São Paulo, Brazil

* Corresponding author: Mariza Pires de Melo, e-mail address: mpmelo@usp.br

ARTICLE INFO

Article history:

Received: April 26, 2018

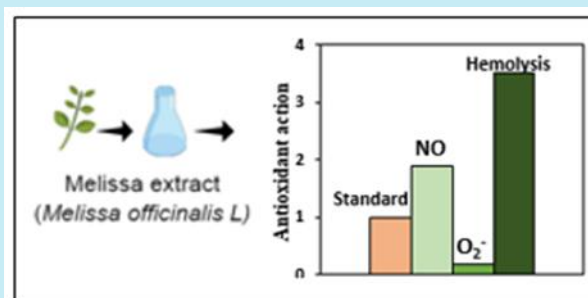
Accepted: September 18, 2018

Published: October 07, 2018

Keywords:

1. adsorbent
2. textile industry
3. isotherms
4. wastewater

ABSTRACT: The aim of the present study was to evaluate *in vitro* antioxidant capacity of Melissa extract (ME) (*Melissa officinalis* L.) and its protective effect on peroxy radical-induced oxidative damage in erythrocytes. ME used in the present study was obtained by rotary evaporation of the crude extract (ethanol:water/dried leaves). Total phenolic and flavonoids determined were 177 ± 13 mg GAE/g dried weight (dw) and 26 ± 3 mg QE/g dw, respectively. Total equivalent antioxidant activities, TEAC in mg TE/g dw, were 61 ± 6 and 512 ± 77 respectively for FRAP assay and DPPH[•] radical-scavenging. The ME acts as an antioxidant on NO and O₂^{•-}, whereas ME exerted a higher antioxidant action on NO scavenging compared to the ascorbic acid (1.9 times). However, the antioxidant capacity of ME on O₂^{•-} was 5.6 times lower than ascorbic acid. The values of hemolysis inhibition from ME (IC₅₀, 2.0 ± 0.5 µg mL⁻¹) were higher than ascorbic acid (IC₅₀, 7 ± 2 µg mL⁻¹). Extract of Melissa was able to eliminate biological free radicals, suggesting a potential to prevent oxidative damage *in vivo*. In fact, the ME exerted protective action on cell membrane lysis *in situ*.



1. Introduction

Melissa officinalis L. (lemon balm) is a plant of the *Lamiaceae* family originated from the Mediterranean, East Asia, Southeast Siberia and North Africa but has adapted throughout the world¹. Studies show the benefits of *M. officinalis* as antioxidant²⁻⁴ which were used for the symptomatic treatment of gastrointestinal disturbances, adjuvant therapy for pain associated to functional dyspepsia, neurological diseases associated with oxidative stress⁵. The rosmarinic acid is the major compound present in the ethanol extract of *M. officinalis*^{3,6,7}. Some properties of *M. officinalis* are related to the high levels of polyphenolic compounds as quercetin, caffeic acid and rosmarinic acid with antioxidant properties^{3,8}.

Antioxidants are compounds with protective action on deleterious effect of reactive species such

as reactive oxygen species (ROS) and reactive nitrogen species (RNS)⁹. Reactive species are atoms or molecules that have high oxidizing power and can be a radical with unpaired electron as superoxide anion (O₂^{•-}), hydroxyl radical (HO[•]) and nitric oxide (NO[•] or NO) or non-radical forms as hydrogen peroxide (H₂O₂) or peroxy nitrite anion (ONOO⁻)^{9,10}. ROS can be formed in the cellular environment primarily as result of aerobic metabolism. Nitric oxide, a natural free radical, whose generation is related to normal physiological parameters; but when combined with ROS has potent pro oxidant effects¹¹.

Exacerbated reactive species in the cellular medium can be due to an unbalanced diet and xenobiotics exposure¹². For food processing the oxygen level, the presence of transition metals and high temperatures are important to the reactive species generation^{11,12}. Macromolecules oxidation

by reactive species can cause serious problems in biological systems by ultracellular damage or in food industry by off flavor, changes in nutritional properties and shelf life; so, the use of antioxidants is an important mechanism against reactive species. In recent years the interest for natural antioxidant has intensified for food manufactures and both human and animal diet^{13, 14}. Different species of herbs have been investigated by the chemical composition, antioxidant activity and antimicrobial action, among them *M. officinalis*.

Antioxidant activity can be evaluated by radical scavenging using non-biological radicals such as DPPH[•] (2,2-diphenyl-1-picrylhydrazyl) and ABTS^{•+} (2,2'-azino-bis-3-ethylbenzthiazoline)¹⁵. However, recently, radicals with biological characteristics as O₂^{•-} and NO have been employed to evaluate antioxidant activity¹⁶. Thermal decomposition of AAPH (2,2'-azobis-2-amidinopropane dihydrochloride) *in vitro* generates peroxy radical that has been used to verify the antioxidant activity against oxidative erythrocytes damage induced by this radical¹⁷. Reactive species such as peroxy radical and others as O₂^{•-} and NO are important for antioxidant assays by simulating a biological process.

The aim of this study was to evaluate the antioxidant activity of extract of *Melissa officinalis* L. on biological systems. For this purpose the aqueous *M. officinalis* extract obtained by ethanol:water (70:30) extraction was used to determinate: *i*) total phenolic by Folin-Ciocalteu method and total flavonoids by aluminum chloride reaction; *ii*) antioxidant activity on non-biological species as ferric ion reducing (FRAP assay) and DPPH[•] scavenging; *iii*) antioxidant activity on free radical with biological characteristics, O₂^{•-} and NO scavenging and *iv*) antioxidant activity on hemolytic AAPH-induced.

2. Materials and methods

2.1 Plant and chemicals

Dried leaves of *M. officinalis* were acquired from Florian (Piracicaba, São Paulo, Brazil). All chemicals compounds were obtained from Sigma-Aldrich (St. Louis, EUA).

2.2 Obtainment of Extract

Dried leaves of *Melissa officinalis* were micronized using a micro mill Willye (TE-648, Tecnal) and stored in amber vial. Micronized sample (10 g) was subjected to lipids removal using

n-hexane (300 mL) on Soxhlet extractor for 6 h¹⁸. Subsequently, the bioactive compounds from each sample was extracted with ethanol:water (70:30, v:v) by stirring (170 rpm) (Shaker TE-420, Tecnal), at 25 °C for 24 h, in the dark. After extraction, the solution was centrifuged for 10 min at 4000 rpm (Centrifuge CT-500, Cientec), filtered Whatman no.1 (11 µM) and the solvent was evaporated under reduced pressure with the temperature not exceeding 50 °C (rotary evaporator SL-126, Solab). The concentrated extract was diluted in ultrapure water, sonicated 3 times for 20 s at 90 Hz (ultrasonic cell disrupter, UNIQUE) and centrifuged at 4000 rpm for 5 min. The supernatant was frozen and freeze-dried (Lyophilizer K-202, Liobras) and finally, the sample was resuspended in ultrapure water and used in all assays. To assay with cells the final extract concentration was adjusted to 10 mM phosphate buffer saline, pH 7.4, (PBS). Dry weight (dw) of aqueous extract was evaluated for results expression. The procedure described above was performed in triplicate (n=3).

2.3. Estimation of total phenolic and total flavonoids

Total phenolics were estimated using Folin-Ciocalteu reagent¹⁹. In this technique, the extract was pre-incubated with 10% (v/v) Folin-Ciocalteu reagent for 2 min and 7.5% (w/v) sodium carbonate was added. After 1 h at 25 °C, absorbance at 760 nm was measured in a spectrophotometer (DU-800, Beckman Coulter®). Assays were performed in triplicate and results were expressed as mg of gallic acid equivalents (GAE)/g dw, using a standard curve of gallic acid (0.5 to 6.0 µg mL⁻¹).

Total flavonoids were carried in accordance with the colorimetric method²⁰. Assay was performed in ethanol:water 70:30 (v:v) in the presence of 2% (w/v) aluminum chloride and extract. Absorbance at 415 nm was determinate, after 40 min of incubation at 25 °C in the dark, using a spectrophotometer (DU-800, Beckman Coulter®). Assays were performed in triplicate and results were expressed in mg of quercetin equivalent (QE)/dw, using a standard curve of quercetin (0.6 to 9.6 µg mL⁻¹).

2.4. Ferric reducing antioxidant power (FRAP) assay

The reduction power of extract on ferric ion was described previously²¹. The reaction between extract and FRAP reagent produces a blue compound and absorbance was measured at 593

nm (DU-800, Beckman Coulter®). FRAP reagent was prepared by mixing acetate buffer (300 mM, pH 3.6), 10 mM tripiridilriazine in 40 mM HCl, and 20 mM FeCl₃ at ratio 10:1:1 (v:v:v). A standard curve was prepared with Trolox (0.63 to 3.78 µg mL⁻¹). Assays were performed in triplicate and results were expressed as mg trolox equivalente (TE)/g dw.

2.5. Radical DPPH[•] scavenging

Antioxidant activity of extract on DPPH[•] radical (2,2-diphenyl-1-picryl-hidrazil) was described above²². A methanol solution of DPPH[•] (65 mM) and extract at different concentrations (2.5 to 16.5 mg mL⁻¹) were used to determine the EC₅₀ (concentration required to reduce 50% of DPPH[•] inhibition). A control assay was performed in the absence of extract to obtain the initial absorbance at zero time. After 3 h of incubation at 25 °C, the absorbance at 515 nm was determined (DU-800, Beckman Coulter®). The antioxidant activity was assessed by reduction of absorbance value from DPPH[•] compared to the initial absorbance from control assay. The results were expressed as inhibition percentage of DPPH[•] in Equation 1. Assays were performed in triplicate and results were expressed as mean ± standard deviation mg TE/g dw, calculated from a standard Trolox curve with concentrations 0.32 to 6.3 mg mL⁻¹. EC₅₀ values were expressed in mg mL⁻¹ of extract.

$$DPPH^{\bullet} \text{ inhibition } (\%) = [1 - (A_A / A_{C_0})] \times 100 \quad (1)$$

where: A_{C0} = absorbance at 515 nm from control assay at initial time; A_A = absorbance at 515 nm from assay in the presence of extract after 3 h of incubation.

2.6. Superoxide anion (O₂^{•-}) and nitric oxide (NO) scavenging

The antioxidant activity on O₂^{•-} was determined according to the methodology proposed previously^{8, 23, 24}. The assay used NADH (166 µM), NBT (43 µM), PMS (2.7 µM) and extract at different concentrations (20 to 600 µg mL⁻¹). All reagents were prepared in PBS. After incubation for 2 min at 25 °C, the absorbance was determined at 540 nm on microplate reader (Thermo Scientific Uniscience®). A control assay (without extract) was performed under the same conditions. Inhibition percentage of O₂^{•-} is described in Equation 2. Assays were performed in triplicate

and results were expressed as mean ± standard deviation as inhibition percentage compared to control assay. Ascorbic acid, as standard antioxidant was used in similar conditions.

$$O_2^{\bullet-} \text{ inhibition } (\%) = [1 - (A_A / A_{C_0})] \times 100 \quad (2)$$

where: A_{C0} = absorbance at 540 nm from control assay; A_A = absorbance at 540 nm from assay in the presence of extract.

For nitric oxide (NO) assay was used the proposed method²⁵, with modifications^{8, 26}. Assay performed in PBS containing 10 mM sodium nitroprusside and extract (2.5 to 100 µg mL⁻¹) were incubated at 25 °C for 3 h. Control assay (without extract) was performed under the same conditions, when 100% nitrite formation was observed. Each 1 h, aliquot from each assay was transferred to 96-well plate containing sulfanilamide (1%, w/v). After 5 min, N-(1-Naphthyl)ethylenediamine dihydrochloride (0.1%, w/v) has been added, incubated for 5 min and absorbance at 540 nm evaluated using a microplate reader (Thermo Scientific Uniscience®). The concentration of sodium nitrite (µmol L⁻¹) in the assays was calculated from a standard curve of sodium nitrite (1.56 to 100 µmol L⁻¹). The NO inhibition percentage by the extract was determined after 2 h of incubation and was calculated relative to the control assay (Equation 3). Assays were performed in triplicate and results were expressed as mean ± standard deviation. Ascorbic acid, as standard antioxidant was used in similar conditions.

$$\text{Inhibition NO } (\%) = [1 - (A_A / A_{C_0})] \times 100 \quad (3)$$

where: A_{C0} = absorbance at 540 nm from control assay; A_A = absorbance at 540 nm from assay in the presence of extract.

2.7. Protective effect on hemolytic AAPH-induced in human erythrocytes

To evaluate the extract action on hemolysis induced by AAPH was employed the method described above^{8, 27, 28}. Human erythrocytes, from venous blood, were obtained from healthy and nonsmokers people using vacutainer tubes containing ethylenediamine tetraacetic acid (EDTA). The cell suspension was prepared according to Gião *et al.*¹⁷ and this suspension was kept at 4 °C and used within 4 h. The volunteers

signed consent and informed, previously approved by the Local Committee of Ethics in Human Research (number: 493.382).

The erythrocytes suspensions (1%) were incubated for 30 min in the absence (control assay) as well in the presence of the extract (0.25 to 15 mg mL⁻¹) at 37 °C under agitation at 100 rpm (shaker TE - 420 Tecnal®). So, each assay received 5 mmol L⁻¹. AAPH and the incubation proceeded for 6 h. Simultaneous, assays in the absence of AAPH were performed, under same conditions, to evaluate spontaneous hemolysis; the effect of extract alone on cell lyses was also tested. The complete hemolysis (100%) was established by incubating erythrocytes (1%) in water at 37 °C for 10 min. Hemolysis was measured, at each 1 h, by hemoglobin absorbance in the extracellular medium at 540 nm using a microplate reader (Thermo Scientific Uniscience®). Assays were performed in duplicate and the results expressed as percentage of hemolysis according to Equation 4. The percentage of hemolysis inhibition related to the control assay was obtained according to Equation 5. Ascorbic acid, as standard antioxidant was used in similar conditions.

$$\text{Hemolysis (\%)} = (A_A / A_{100\%}) \times 100 \quad (4)$$

$$\text{Hemolysis inhibition (\%)} = [1 - (A_A / A_C)] \times 100 \quad (5)$$

where: A_A = absorbance at 540 nm from assay in the presence of extract; A_{100%} = absorbance at 540 nm from complete hemolytic assay (100%); A_C = absorbance at 540 nm from control assay.

2.8 Statistic analysis

The data were evaluated by analysis of variance (ANOVA), t-test and Tukey's test for comparison of means, with a significance level of 5%, using Minitab® software 16.2.2 (2010 Minitab Inc.).

3. Results and discussion

3.1 Total phenolic and flavonoid contents and antioxidant activity against ferric reducing power (FRAP) and free radical scavenging (DPPH, NO and O₂^{•-})

The present study determined the antioxidant properties of *M. officinalis* and its action on reactive species. Total phenolic and flavonoids content on ME, evaluated by spectrophotometry, were 177 ± 13 mg GAE/g dw and 26 ± 3 mg QE/g

dw, respectively. Results expressed by mean and standard deviation (n=3). *Lamiaceae* family, including the *M. officinalis* species, has been studied for polyphenolic presence and total antioxidant properties². Results from Folin-Ciocalteu assays reflect the reducing power of the sample, including total polyphenols and other compounds such as: aromatic amines; ascorbic acid; sugars; organic acids and some inorganic compounds¹². However, Folin-Ciocalteu method has been used to estimate total phenolic compounds. Folin-Ciocalteu values, in the present study, were similar the ethanolic (98%) *M. officinalis* extract (175 ± 11 mg GAE/g of dry extract) and slightly higher for the content of flavonoid (54 ± 4 mg catechin equivalent/g of dried extract)⁴. However, lower values using ethanolic (80%) *M. officinalis* extract by Folin-Ciocalteu assay (13.2 mg GAE/100 g dw) were found⁶. Another study showed the total polyphenols around 69.49–76.43 mg GAE/g dry plant and total flavonoids 7.0–10.0 mg QE/g dry plant from ethanolic (70%) *M. officinalis* extract, dependent of the harvesting period and hour⁷.

Fernandes *et al.*² evaluated six families of aromatic herbs and the *Lamiaceae* family showed higher values of total phenolic by Folin-Ciocalteu assay, compared to other families. These authors found 42.86 mg GAE/g dw for ME using acetone:water:acetic acid (70:28:2) as extractor solvent. So, aqueous extracts of *M. officinalis* prepared by decoction were 1245 mg GAE/g dw and by infusion mode were 267 mg GAE/g dw³. Rababah *et al.* (2015)²⁹ studying methanolic extract from leaves of *M. officinalis* found 303.2 mg GAE/100 g fresh plant and 252.9 mg of catechin equivalent/100 g fresh plant. Thus, several factors may affect the absolute values of total phenolics and flavonoids contents, including genotype, growing conditions, parts tested, time of taking sample and extraction methods. Recently, the content of total flavonoids by spectrophotometric method was evaluated in different plants extracts and *M. officinalis* specie showed high flavonoids content³⁰.

In the present study, the obtained total antioxidant activity of ME measured by FRAP assay was 61 ± 6 mg TE/g dw, result expressed by mean and standard deviation (n=3). A proportional decrease in the absorbance *versus* the sample concentration was observed (data not show). For DPPH radical scavenging, 3 h were necessary to reach an absorbance plateau, thus ensured that the

derivative zero of the absorbance by time (Figure 1A). Non-linear decay behavior of the absorbance versus time using some extract concentrations was observed, the stability achieved after 3 h of reaction. Dose-response on DPPH[•] radical scavenging by extract after 3 h of reaction was studied (Figure 1B). High linear correlation coefficient ($r^2 = 0.9935$) was found for DPPH[•] scavenging and extract concentration (0.5-17.0 $\mu\text{g mL}^{-1}$). Similar behavior was presented by Trolox, a standard antioxidant, at concentration of 1.0-6.0 $\mu\text{g mL}^{-1}$ ($r^2 = 0.9826$) (Figure 1B). IC₅₀ values were $9 \pm 1 \mu\text{g mL}^{-1}$ and $5.5 \pm 0.2 \mu\text{g mL}^{-1}$ to extract and Trolox, respectively. These results suggest that the ME has antioxidant activity on non-biological radical DPPH[•], but slightly less efficient than Trolox. Total antioxidant activity of ME measured by DPPH[•] scavenging was $512 \pm 77 \text{ mg TE/g dw}$, as mean and standard deviation.

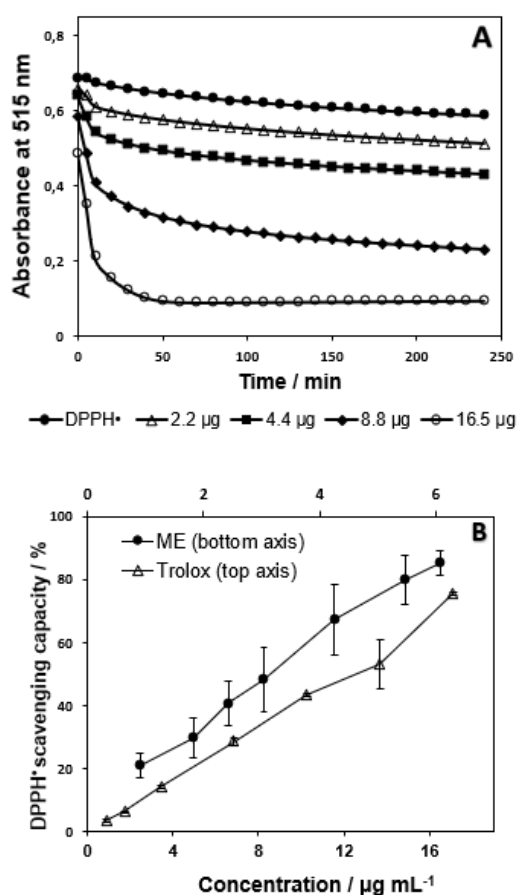


Figure 1. Antioxidant activity of ME on DPPH[•] scavenging. (A) Absorbance versus reaction time in absence of extract (only DPPH[•]) and presence of extract (2.2, 4.4, 8.8, 15.5 μg). (B) DPPH[•] scavenging by ME (0.5 at 17.0 $\mu\text{g mL}^{-1}$) and by Trolox (1.0 at 6.0 $\mu\text{g mL}^{-1}$), after 3 h of incubation mean \pm standard deviation for assay made in triplicate from 3 extractions ($n=3$).

FRAP assay is based on the ability of different antioxidants, including phenolics, to reduce Fe^{3+} to Fe^{2+} in the presence of FRAP-reagent, forming a blue chromophore. Results obtained here indicating that ME had effective reducing power and showed similar characteristic when compared to the standard ascorbic acid. Total antioxidant activity of ME measured by FRAP assay was $61 \pm 6 \text{ TE/g dw}$, in the present study, contrasting with the results found in previous study using another extractor solvent (464.8 $\mu\text{mol TE/g dw}$ that correspond 117 mg TE/g dw)². In the present study, FRAP assay corroborates the Folin-Ciocalteu values and can indicate high reducing power of the sample, suggesting great antioxidant potential from the ME. Reducing power can be associated with antioxidant activity of plant extract³¹. The reduction power indicates that the antioxidant compounds present in the sample are electron donors and can react with free radicals to stabilize and block chain reactions¹.

Antioxidant compounds can act on free radicals by scavenging mechanisms, which may be attributed to its hydrogen and/or electron donating; thus, they might prevent reactive radical species from reaching biomolecules such as lipoproteins, polyunsaturated fatty acids, DNA, amino acids, proteins and food systems³². It is well described that DPPH[•] radical is a good model for assessing antioxidant activity²². Here, *M. officinalis* showed a concentration-dependent DPPH[•] radical scavenging. The DPPH[•] radical assay is based on the reduction of DPPH[•] radical to a non-radical compound by antioxidant agents, e.g. *M. officinalis* extract. In the present study, the extract showed a potent action on the DPPH[•] scavenging which IC₅₀ is similar to other studies of aqueous and methanol extract of *M. officinalis* (18.74 $\mu\text{g mL}^{-1}$ and 13.74 $\mu\text{g mL}^{-1}$, respectively)³³.

Studies with aqueous ME exhibited IC₅₀ to DPPH[•] scavenging from 1.53-1.62 $\mu\text{g mL}^{-1}$ ⁷. Results presented here show values 10 \times higher than antioxidant activity of ME against DPPH[•] radical scavenging found previously (5.57 g TE/100 g dw, that correspond 55.7 mg TE/g dw)². There is a large variation in the absolute values for the DPPH[•] radical scavenging by ME. However, this found suggests that the ME can eliminate free radicals at physiological pH and can be of beneficial interest in preservation of biological systems, where free radical mediates some reactions including lipid oxidation. DPPH[•] radical-scavenging from ME ethanolic (80%) shows IC₅₀

equal $48.76 \mu\text{g mL}^{-1}$, which is less efficient than ascorbic acid ($6.64 \mu\text{g mL}^{-1}$)³⁴. Antioxidant activity of ME on DPPH[•] radical scavenging was 3.03-6.34 $\mu\text{mol Trolox/mL}$ of water extract, depending on the extraction procedure as temperature and ultrasound bath³⁵.

To nitric oxide assay, the antioxidant activity of extract was measured by decrease of nitrite (NO_2^-) concentration over reaction time (Figure 2A). Melissa extract activity on NO radical scavenging was estimated by the decreasing of NO_2^- concentration. After 3 h of reaction, NO inhibition by extract in different concentrations (0.5-100 $\mu\text{g mL}^{-1}$)

mL^{-1}) was studied (Figure 2B). However, a good linear correlation coefficient ($r^2 = 0.9895$) was found for NO radical scavenging and extract concentration (0.5-17.0 $\mu\text{g mL}^{-1}$). Similar characteristic was found by ascorbic acid evaluated in a concentration range of 0.5-200 $\mu\text{g mL}^{-1}$ (Figure 2B); and good linear correlation coefficient ($r^2 = 0.9901$) between this radical scavenging and ascorbic acid concentration (0.5-25 $\mu\text{g mL}^{-1}$) was observed. So, IC_{50} value for the ME ($35 \pm 12 \mu\text{g mL}^{-1}$) was better than ascorbic acid ($68 \pm 17 \mu\text{g mL}^{-1}$).

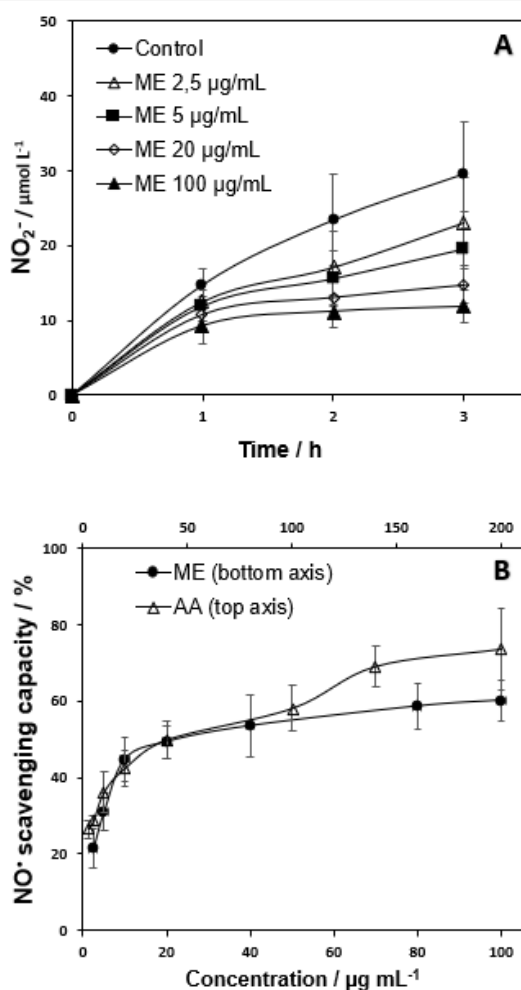


Figure 2. Antioxidant activity of ME on NO scavenging. (A) NO_2^- concentration *versus* reaction time in the absence of extract (control) and the presence of extract (2.5 at 100 $\mu\text{g mL}^{-1}$). (B) NO scavenging by ME (2.5 at 100 $\mu\text{g mL}^{-1}$) and by ascorbic acid (AA, 2.5 at 200 $\mu\text{g mL}^{-1}$), after 3 h of incubation. Mean \pm standard deviation for assay made in triplicate from 3 extractions ($n=3$).

The NO radical-scavenging by antioxidants is performed by the quantification of nitrite ions (NO_2^-) generated by reaction between NO and molecular oxygen²⁵. However, the antioxidant action of ME on NO can be deduced by the low

concentration of NO_2^- . Other studies show that plant extracts were effective for NO scavenging, when IC_{50} values from 18 different plant species on NO inhibition were 51-604 $\mu\text{g mL}^{-1}$ ¹⁰. So, IC_{50} for the ME was $35 \pm 12 \mu\text{g/mL}$ in present study.

Normally, the reaction mechanism to NO radical scavenging by plants extracts involves phenolic compounds³⁶. ME has shown various phenolic compounds such as rosmarinic acid and others¹⁰, in fact, these compounds can be related to the NO radical scavenging. The NO is a natural compound produced *in vivo* by variety of cells and is an important bio-regulatory molecule with several physiological functions^{11,37}. However, under oxidative stress this reactive species combines with other reactive species to produce more toxic effects¹¹. Therefore, the scavenging effect of ME was assessed against this radical. NO radical scavenging by extract has an interest in human health. It is well known that NO plays an important role in the prevention of various pathologies such as atherosclerosis, ischemia reperfusion, neurodegenerative diseases such as Alzheimer's and Parkinson's disease, cancer and diabetes^{11,37-39}.

A relationship between the concentration of ME and $O_2^{\cdot-}$ inhibition was obtained in 0.5-600 $\mu\text{g mL}^{-1}$ range to extract and 0.5-200 $\mu\text{g mL}^{-1}$ to ascorbic acid (Figure 3). However, linear correlation between $O_2^{\cdot-}$ scavenging and ME extract at 0.5-80 $\mu\text{g mL}^{-1}$ ($r^2 = 0.9781$) was obtained; and for ascorbic acid in the range 0.5-25 $\mu\text{g mL}^{-1}$ ($r^2 = 0.9879$). Therefore, the effect of extract on $O_2^{\cdot-}$ scavenging was 5.6 \times lower than for ascorbic acid, observed, respectively, by IC_{50} values, $247 \pm 43 \mu\text{g mL}^{-1}$ and $44 \pm 18 \mu\text{g mL}^{-1}$.

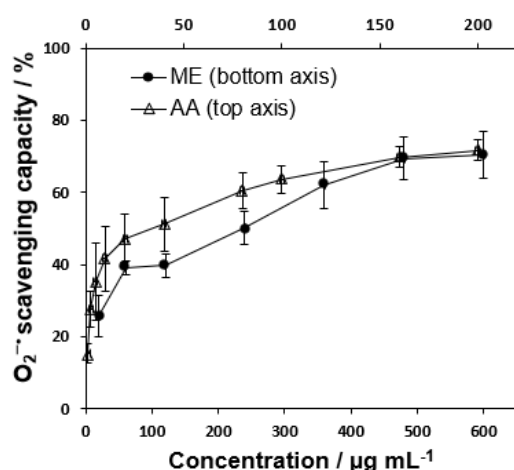


Figure 3. Antioxidant activity on $O_2^{\cdot-}$ scavenging by ME (20 at 600 $\mu\text{g mL}^{-1}$) and by ascorbic acid (AA, 10 at 200 $\mu\text{g mL}^{-1}$). Mean \pm standard deviation for assay made in triplicate from 3 extractions ($n=3$).

The $O_2^{\cdot-}$ radical scavenging determination is based on the formazan chromophore formation by

reaction between this radical and nitro blue tetrazolium, at physiological pH; antioxidant compound reacts with $O_2^{\cdot-}$ and chromophore formation is inhibited²⁴. In the present study, the $O_2^{\cdot-}$ radical scavenging by ME was 5.6 \times lower than ascorbic acid. Other authors showed IC_{50} variation from 44 to 386 $\mu\text{g mL}^{-1}$ for $O_2^{\cdot-}$ scavenging in aqueous ME from several cultivars³⁰; our results are within the reported range ($247 \pm 43 \mu\text{g mL}^{-1}$).

Recent studies reported that $O_2^{\cdot-}$ radical scavenging by plant aqueous extracts can be due to the presence of hydroxyl groups in phenolic compounds³⁸. The $O_2^{\cdot-}$ is an important reactive oxygen species *in vivo* and can generate highly toxic species through reactions with other reactive species or by enzymatic reactions or metal catalyzed processes. The $O_2^{\cdot-}$ mediated oxidative stress and it is believed to be involved in pathogenesis disorders such as diabetes mellitus, Alzheimer's and Parkinson's diseases³⁹.

3.2. Anti-hemolytic action on AAPH-induced lysis

Results from action of ME on hemolysis inhibition are shown in Figure 4. The hemolysis percentage induced by AAPH has a sigmoidal characteristic over time (Figure 4A). When low hemolysis percentages up to 2 h and after 5 h of incubation 30% hemolysis was seen, compared to 100% hemolysis induced by water. However, MEs at 1-10 $\mu\text{g mL}^{-1}$ were antihemolytic on AAPH-induced lysis following a dose-dependent characteristic. No hemolysis by the extract (10 $\mu\text{g mL}^{-1}$) alone, in the absence of AAPH, was detected. Figure 4B shows dose-dependence of antioxidant concentration and inhibition hemolysis percentage after 4 h of erythrocytes incubation in the presence of extract or ascorbic acid in a concentration range from 0.5 to 15 $\mu\text{g mL}^{-1}$. Linear correlation between hemolysis inhibition and antioxidant concentration (0.5-8 $\mu\text{g mL}^{-1}$) showed $r^2 = 0.9987$ and $r^2 = 0.7899$ for Melissa extract and ascorbic acid, respectively. IC_{50} values indicated that the extract was more efficient in protecting red blood cell lysis, since IC_{50} for extract was $2.0 \pm 0.5 \mu\text{g mL}^{-1}$ and for ascorbic acid $7 \pm 2 \mu\text{g mL}^{-1}$.

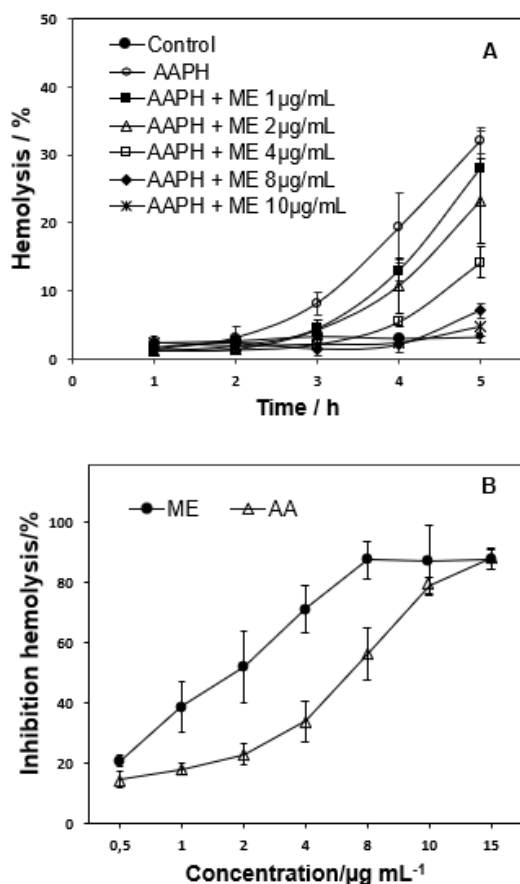


Figure 4. Antihemolytic action of ME. (A) Percentage of AAPH-induced hemolysis over time evaluated in absence and presence of ME (1 at 10 $\mu\text{g mL}^{-1}$), in relation with 100% hemolysis induced by water. A control test (only erythrocytes) in the absence of ME and AAPH was made (control). (B) Hemolysis inhibition by ME and ascorbic acid (AA, 0.5 at 15 $\mu\text{g mL}^{-1}$) after 4 h of incubation, in relation with control assay (absence of antioxidant). Mean \pm standard deviation for assay made in triplicate from 3 extractions ($n=3$).

AAPH decomposition in the presence of oxygen generates peroxy radical causing oxidative damage in cell membranes. Erythrocytes are very susceptible to oxidative damage by the high content of polyunsaturated fatty acids in their membranes and high cell concentrations of oxygen and hemoglobin²⁸. Thus, peroxy radical, generated by the decomposition of AAPH, attacks cell membranes of erythrocytes induced by lipid peroxidation and protein conformational changes, leading to hemolysis^{8, 40}. Similarly, in the present study, it was observed effects of peroxy radicals initiated by AAPH on human erythrocytes lyses. A lag phase in the progress curve of hemolysis during incubation with AAPH was observed, suggesting a

complex mechanism in the oxidative damage process. Our findings indicated that the antihemolytic effect was more efficient by ME than by ascorbic acid. In addition, flavonoid compounds showed protective effect against hemolysis induced by AAPH in erythrocytes of rats⁴¹. The possible mechanisms of these protective effects of flavonoid-rich fractions may be through their radical scavenging, metal chelating and reducing power activities⁴¹.

4. Conclusions

The antioxidant action found in this study clearly demonstrates that ME is able to eliminate synthetic and naturally occurring free radicals, suggesting its potential to prevent oxidative damage *in vivo* as well as in foodstuffs. In fact, the ME exerted protective action on erythrocytes membrane lysis.

5. Acknowledgments

The authors thank Prof. Dr. Olga Maria M. de Faria-Oliveira for her collaboration in the standardization of the techniques employed in the present study.

6. References

- [1] Chanda, S., Dave, R., *In vitro* models for antioxidant activity evaluation and some medicinal plants possessing antioxidant properties: An overview, *Afr. J. Microbiol. Res.* 3 (2009) 981-996.
- [2] Fernandes, R. P. P., Trindade, M. A., Tonin, F. G., Lima, C. G., Pugine, S. M. P., Muneakata, P. E. S., Lorenzo, J. M., De Melo, M. P., Evaluation of antioxidant capacity of 13 plant extracts by three different methods: cluster analyses applied for selection of the natural extracts with higher antioxidant capacity to replace synthetic antioxidant in lamb burgers, *J. Food Sci. Technol.* 53 (2016) 451-460. <https://doi.org/10.1007/s13197-015-1994-x>.
- [3] Sentkowska, A., Biesaga, M., Pyrzynska, K., Polyphenolic Composition and Antioxidative Properties of Lemon Balm (*Melissa officinalis* L.) Extract Affected by Different Brewing Processes, *Int. J. Food Prop.* 18 (2015) 2009-2014. <https://doi.org/10.1080/10942912.2014.960932>.

- [4] Lin, J. T., Chen, Y. C., Lee, Y. C., Rolis Hou, C. W., Chen, F. L., Yang, D. J., Antioxidant, anti-proliferative and cyclooxygenase-2 inhibitory activities of ethanolic extracts from lemon balm (*Melissa officinalis* L.) leaves, *LWT-Food Sci. Technol.* 49 (2012) 1-7. <https://doi.org/10.1016/j.lwt.2012.04.009>.
- [5] Zemmouri, H., Ammar, S., Boumendjel, A., Messarah, M., Feki, A. E., Bouaziz, M., Chemical composition and antioxidant activity of *Borago officinalis* L. leaf extract growing in Algeria, *Arabian J. Chem.* article in press (2014). <https://doi.org/10.1016/j.arabjc.2014.11.059>.
- [6] Wojdylo, A., Oszmianski, J., Czemerys, R., Antioxidant activity and phenolic compounds in 32 selected herbs, *Food Chem.* 105 (2007) 940-949. <https://doi.org/10.1016/j.foodchem.2007.04.038>.
- [7] Duda, S. C., Mărghițaș, L. A., Dezmirean, D., Duda, M., Mărgăoan, R., Bobiș, O., Changes in major bioactive compounds with antioxidant activity of *Agastache foeniculum*, *Lavandula angustifolia*, *Melissa officinalis* and *Nepeta cataria*: Effect of harvest time and plant species, *Int. J. Food Prop.* 77 (2015) 499-507. <https://doi.org/10.1016/j.indcrop.2015.09.045>.
- [8] Velloso, J. C. R., Regaini L. O., Khalil, N. M., Bolzani, V. S., Khalil O. K., Manente, F. A., Netto H. P., Faria-Oliveira O. M. M., Antioxidant and cytotoxic studies for kaempferol, quercetin and isoquercetin, *Eclet. Quim.* 36 (2011) 7-19. <https://doi.org/10.1590/S0100-46702011000200001>.
- [9] Halliwell, B., Gutteridge, J., *Free Radicals in Biology and Medicine*, New York: Oxford University Press Inc.; 2nd ed.; 2007, ch 3.
- [10] Conforti, F., Marrelli, M., Carmela, C., Menichini, F., Valentina, P., Uzunov, D., Statti, G. A., Duez, P., Menichini, F., Bioactive phytonutrients (omega fatty acids, tocopherols, polyphenols), in vitro inhibition of nitric oxide production and free radical scavenging activity of non-cultivated Mediterranean vegetables, *Food Chem.* 129 (2011) 1413-1419. <https://doi.org/10.1016/j.foodchem.2011.05.085>.
- [11] Valko, M., Leibfritz, D., Moncol, J., Cronin, M. T. D., Mazur, M., Telser, J., Free radicals and antioxidants in normal physiological functions and human disease, *Int. J. Biochem. Cell Biol.* 39 (2007) 44-84. <https://doi.org/10.1016/j.biocel.2006.07.001>.
- [12] Prior, R. L., Wu, X., Schaich, K., Standardized methods for the determination of antioxidant capacity and phenolics in foods and dietary supplements, *J. Agric. Food Chem.* 53 (2005) 4290-4302. <https://doi.org/10.1021/jf0502698>.
- [13] Carocho, M., Ferreira, I. C. F. R., A review on antioxidants, prooxidants and related controversy: Natural and synthetic compounds, screening and analysis methodologies and future perspectives, *Food Chem. Toxicol.* 51 (2013) 15-25. <https://doi.org/10.1016/j.fct.2012.09>.
- [14] Vargas, F. C., Arantes-Pereira, L., Costa, P. A., De Melo, M. P., Sobral, P. J. A., Rosemary and Pitanga Aqueous Leaf Extracts On Beef Patties Stability under Cold Storage, *Braz. Arch. Biol. Technol.* 59 (2016) 1-10. <https://doi.org/10.1590/1678-4324-2016160139>.
- [15] Floegel, A., Kim, D. O., Chung, S. J., Koo, S. I., Chun, O. K., Comparison of ABTS/DPPH assays to measure antioxidant capacity in popular antioxidant-rich US foods, *J. Food Compos. Anal.* 24 (2011) 1043-1048. <https://doi.org/10.1016/j.jfca.2011.01.008>.
- [16] López-Alarcón, C., Denicola, A., Evaluating the antioxidant capacity of natural products: A review on chemical and cellular-based assays, *Anal. Chim. Acta* 763 (2013) 1-10. <https://doi.org/10.1016/j.aca.2012.11.051>.
- [17] Gião, M. S., Leitão, I., Pereira, A., Borges, A. B., Guedes, C. J., Fernandes, J. C., Belo, L., Santos-Silva, A., Hogg, T. A., Pintado, M. E., Malcata, F. X., Plant aqueous extracts: Antioxidant capacity via haemolysis and bacteriophage P22 protection. *Food Control.* 21 (2010) 633-638. <https://doi.org/10.1016/j.foodcont.2009.08.014>.
- [18] Virost, M., Tomao, V., Colnagui, G., Visinoni, F., Chemat, F., New microwave-integrated Soxhlet extraction. An advantageous tool for the

- extraction of lipids from food products, *J. Chromatogr. A.* 1174 (2007) 138-144. <https://doi.org/10.1016/j.chroma.2007.09.067>.
- [19] Singleton, V. L., Rossi Junior, J. A., Colorimetry of total phenolics with phosphomolybdic-phosphotungstic acid reagents, *Am. J. Enol. Vitic.* 16 (1965) 144-158.
- [20] Miliuskas, G., Venskutonis, P. R., van Beek, T. A., Screening of radical scavenging activity of some medicinal and aromatic plant extracts, *Food Chem.* 85 (2004) 231-237. <https://doi.org/10.1016/j.foodchem.2003.05.007>.
- [21] Benzie, I. F. F., Strain, J. J., The Ferric Reducing Ability of Plasma (FRAP) as a Measure of "Antioxidant Power": The FRAP Assay, *Anal. Biochem.* 239 (1996) 70-76. <https://doi.org/10.1006/abio.1996.0292>.
- [22] Brand-Williams, W., Cuvelier, M. E., Berset, C., Use of a free radical method to evaluate antioxidant activity, *LWT-Food Sci. Technol.* 28 (1995) 25-30. [https://doi.org/10.1016/S0023-6438\(95\)80008-5](https://doi.org/10.1016/S0023-6438(95)80008-5).
- [23] Valentão, P., Fernandes, E., Carvalho, F., Andrade, P. B., Seabra, R. M., Bastos, M. L., Antioxidant activity of *Centaurium erythraea* infusion evidenced by its superoxide radical scavenging and xanthine oxidase inhibitory activity, *J. Agric. Food Chem.* 49 (2001) 3476-3479. <https://doi.org/10.1021/jf001145s>.
- [24] Orak, H. H., Isbilir, S. S., Yagar, H., Determination of antioxidant properties of lyophilized olive leaf water extracts obtained from 21 different cultivars, *Food Sci. Biotechnol.* 21 (2012) 1065-1074. <https://doi.org/10.1007/s10068-012-0138-6>.
- [25] Marcocci, L., Maguire, J. J., Droy-Lefaix, M. T., Packer, L., The nitric oxide-scavenging properties of ginkgo biloba extract EGb 761, *Biochem. Biophys. Res. Commun.* 201 (1994) 748-755. <https://doi.org/10.1006/bbrc.1994.1764>.
- [26] Pooja, P. S., Samanta, K. C., Garg, V., Evaluation of nitric oxide and hydrogen peroxide scavenging activity dalbergia sissoo roots, *Pharmacophore* 1 (2010) 77-88. <http://www.pharmacophorejournal.com>.
- [27] Simão, A. N. C., Suzukawa, A. A., Casado, M. F., Oliveira, R. D., Guarnier, F. A., Cecchini, R., Genistein abrogates pre-hemolytic and oxidative stress damage induced by 2,2'-Azobis (Amidinopropane), *Life Sci.* 78 (2006) 1202-1210. <https://doi.org/10.1016/j.lfs.2005.06.047>.
- [28] Yang, H. L., Chen, S. C., Chang, N. W., Chang, J. M., Lee, M. L., Tsai, P. C., Fu, H. H., Kao, W. W., Chiang, H. C., Wang, H. H., Hseu, Y. C., Protection from oxidative damage using *Bidens pilosa* extracts in normal human erythrocytes, *Food Chem. Toxicol.* 44 (2006) 1513-1521. <https://doi.org/10.1016/j.fct.2006.04.006>.
- [29] Rababah, T. M., Al, U., Datt, M., Alhamad, M., Al-Mahasneh, M., Ereifej, K., Andrade, J., Altarifi, B., Almajwal, A., Yang, W., Effects of drying process on total phenolics, antioxidant activity and flavonoid contents of common mediterranean herbs, *Int. J. Agric. & Biol. Eng.* 8 (2015) 145-150. <https://doi.org/10.3965/j.ijabe.20150802.1496>.
- [30] Dudek, G., Strzelewicz, A., Krasowska, M., Rybak, A., Turczyn, R., A spectrophotometric method for plant pigments determination and herbs classification, *Chem. Pap.* 68 (2014) 579-583. <https://doi.org/10.2478/s11696-013-0502-x>.
- [31] Oktay, M., Gülçin, I., Küfrevioğlu, Ö. I., Determination of in vitro antioxidant activity of fennel (*Foeniculum vulgare*) seed extracts, *LWT-Food Sci. Technol.* 36 (2003) 263-271. [https://doi.org/10.1016/S0023-6438\(02\)00226-8](https://doi.org/10.1016/S0023-6438(02)00226-8).
- [32] Halliwell, B., Gutteridge, J. M. C., Cross, C. E., Free radicals, antioxidants, and human disease: Where are we now? *J. Lab. Clin. Med.* 119 (1992) 598-620. PMID: 1593209.
- [33] López, V., Akerreta, S., Casanova, E., García-Mina, J. M., Cavero, R. Y., Calvo, M. I., In Vitro Antioxidant and Anti-rhizopus Activities of Lamiaceae Herbal Extracts, *Plant. Foods Hum. Nutr.* 62 (2007) 151-155. <https://doi.org/10.1007/s11130-007-0056-6>.
- [34] Kamdem, J. P., Adeniran, A., Boligon, A. A., Klimaczewski, C. V., Elekofehinti, O. O., Hassan, W., Ibrahim, M., Waczuk, E. P., Meinerz, D. F.,

Athayde, M. L., Antioxidant activity, genotoxicity and cytotoxicity evaluation of lemon balm (*Melissa officinalis* L.) ethanolic extract: Its potential role in neuroprotection, *Ind. Crops. Prod.* 51 (2013) 26-34. <https://doi.org/10.1016/j.indcrop.2013.08.056>.

[35] Skotti, E., Anastasaki, E., Kanellou, G., Polissiou, M., Tarantilis, P. A., Total phenolic content, antioxidant activity and toxicity of aqueous extracts from selected Greek medicinal and aromatic plants, *Ind. Crops. Prod.* 53 (2014) 46-54. <https://doi.org/10.1016/j.indcrop.2013.12.013>.

[36] Ebrahimzadeh, M. A., Nabavi, S. F., Nabavi, S. M., Pourmorad, F., Nitric oxide radical scavenging potential of some Elburz medicinal plants, *Afr. J. Biotechnol.* 9 (2010) 5212-5217. <https://doi.org/10.5897/AJB10.101>.

[37] Law, A., Gauthier, S., Quirion, R., Say NO to Alzheimer's disease: the putative links between nitric oxide and dementia of the Alzheimer's type, *Brain Res. Brain Res. Rev.* 35 (2001) 73-96. [https://doi.org/10.1016/S0165-0173\(00\)00051-5](https://doi.org/10.1016/S0165-0173(00)00051-5).

[38] Govindan, P., Muthukrishnan, S., Evaluation of total phenolic content and free radical scavenging activity of *Boerhavia erecta*, *J. Acute. Med.* 3 (2013) 103-109. <https://doi.org/10.1016/j.jacme.2013.06.003>.





[39] Manoharan, S., Guillemin, G. J., Abiramasundari, R. S., Essa, M. M., Akbar, M., Akbar, M. D., The Role of Reactive Oxygen Species in the Pathogenesis of Alzheimer's Disease, Parkinson's Disease, and Huntington's Disease: A Mini Review, *Oxid. Med. Cell Longev.* 2016 (2016) 1-15. <https://doi.org/10.1155/2016/8590578>.

[40] Zou, C. G., Agar, N. S., Jones, G. L., Oxidative insult to human red blood cells induced by free radical initiator AAPH and its inhibition by a commercial antioxidant mixture, *Life Sci.* 69(2001) 75-86. [https://doi.org/10.1016/S0024-3205\(01\)01112-2](https://doi.org/10.1016/S0024-3205(01)01112-2).

[41] Alinezhad, H., Zare, M., Nabavi, S. F., Naqinezhad, A., Nabavi, S. M., Antioxidant, antihemolytic, and inhibitory activities of endemic *Primula heterochroma* against Fe²⁺-induced lipid

peroxidation and oxidative stress in rat brain in vitro, *Pharm. Biol.* 50 (2012) 1391-1396. <https://doi.org/10.3109/13880209.2012.676050>.

Validation of analytical methodology for determination of Personal Care Products in environmental matrix by GC-MS/MS

Tais Cristina Filippe¹, Franciane de Almeida Brehm Goulart¹, Alinne Mizukawa¹, Júlio César Rodrigues de Azevedo¹

¹ Universidade Tecnológica Federal do Paraná (UTFPR), Rua Deputado Heitor Alencar Furtado, 5000, Curitiba, Paraná, Brazil

+ Corresponding author: Tais Cristina Filippe, e-mail address: taisfilippe@gmail.com

ARTICLE INFO

Article history:

Received: December 29, 2017

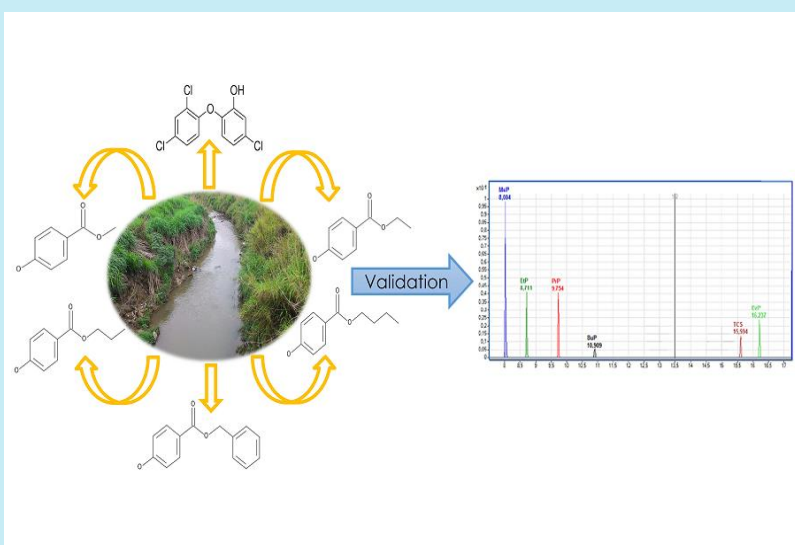
Accepted: September 18, 2018

Published: October 07, 2018

Keywords:

1. environmental analysis
2. chromatography
3. micropollutants

ABSTRACT: The presence of personal care products in the environment is recent and few researches work with the quantification of this class of emerging contaminants in Brazil variety of these products is released into the aquatic environment. The growing interest in these substances occurs mainly because they exhibit biological activity in very low concentrations, which gives a great environmental relevance. The present study aims to validate a methodology and verify its efficiency in the determination of six personal care products, among them parabens and triclosan. The samples were submitted to the solid phase extraction process and were later analyzed by gas chromatography coupled with mass spectrometry for the determination of personal care products. The validation of the methodology used was based on the standards established by the National Health Surveillance Agency. The method showed good recoveries (56 - 117%) and the limits of detection of the method ranged between 0.9 and 14.6 ng L⁻¹, while the limits of quantification were within the 3.1- 48.7 ng L⁻¹. Reproducibility and repeatability, expressed as coefficient of variation, had satisfactory values (<15%). The extraction and quantification method were efficient for the determination of these analytes in water samples.



1. Introduction

Personal care products (PCPs) are used at scale and their presence in aquatic environments has received increasing attention from the scientific community with recent studies indicating the toxic potential to the environment¹⁻³.

PCPs are present in UV filters (benzophenones), preservatives (parabens), antimicrobials (triclosan), fragrances, repellents

among others. One of the most studied PCPs and among the ten organic compounds normally detected in water is triclosan^{4,5}. It has been used in a large number of PCPs, and can be found in soaps, deodorants, body moisturizers, toothpastes and also a component of polymers and fibers⁶. Parabens also comprise a group that is currently under study, most are part of the formulation of various cosmetics and are also used as preservatives in the food industry⁷.

As for the instrumental analytical technique, the most used for the determination of parabens and other classes of contaminants in waters is the chromatography, being able to be used both gas and liquid, both of which can be coupled to different types of detectors to obtain methods even more sensitive and selective⁸. Another analytical method that is being used is the capillary electrophoresis, due to the low cost and the possibility to determine the concentration of the compound of interest directly in the sample, without pre-treatments or previous separations⁹.

The concern of the scientific community with the damages that these contaminants can cause, especially in aquatic environments, the current research has been aimed at implementing and validating new analytical methods that are more sensitive and precise, allowing the advancement of research related to the evaluation of the quality of water resources in terms of micropollutants¹⁰⁻¹².

The aim of this study was validated an analytical methodology applied in the determination of PCPs in surface water by gas chromatography coupled to mass spectrometry (GC-MS/MS).

2. Experimental

2.1 Reagents, solvents and analytical standards

All analytical standards (MeP (99%), EtP (99%), PrP (99%), butylparaben (BuP, 99%), triclosan (97%), N,O-Bis(trimethylsilyl)trifluoroacetamide (BSTFA) + 1% trimethylchlorosilane (TMCS, 98.5%) and solvents were purchased from Sigma Aldrich (Steinheim, Germany). The SPE C18 6 mL cartridges with 1000 mg of adsorbent phase were provided from Hexis (Jundiaí, SP). The solvents used in sample preparation and chromatography analysis (methanol, hexane, ethyl acetate, acetonitrile, and acetone), were HPLC-grade, from Sigma Aldrich. Merck (Darmstadt, Germany) supplied hydrochloric acid (HCl, analytical grade) and porosity membranes of cellulose acetate were acquired from Millipore (Billerica, MA). Ultrapure water was prepared using a water purification system from Millipore. N₂ and He gases (purchased

from White Martins, Rio de Janeiro, Brazil) were 5.0 purity grade.

2.2 Extraction

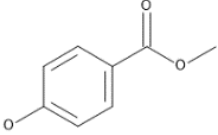
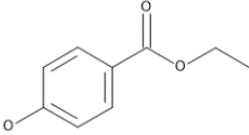
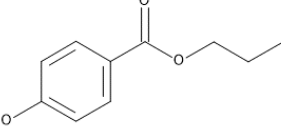
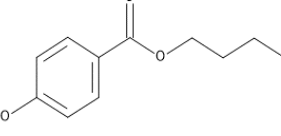
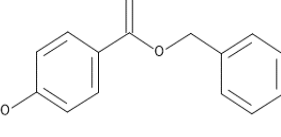
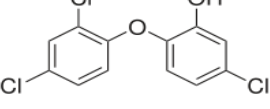
The PCPs analyzed in this work are present in Table 1, with their respective classes. These compounds were chosen because of the large production and the wide consumption by the population in general.

In order to apply the methodology to the real matrices, samples were collected at seven points in the Palmital river basin, located in the state of Paraná, specifically in the Metropolitan Region of Curitiba (MRC). Surface water samples were collected in four campaigns performed in October/2016, February/2017, May/2017 and July/2017.

The methodology used for the extraction of PCPs was adapted from Ide, Cardoso e Marques (2013)¹³. First, 1 liter of sample was filtered on 0.45 µm cellulose acetate membranes to remove particulate matter. Then the pH of the sample was adjusted to 3 with addition of HCl 6 mol L⁻¹. For the solid phase extraction (SPE), C18 (Agila SampliQ 1000 mg - C18 6 mL) cartridges were preconditioned with 6 mL of hexane, 6 mL of acetone, 6 mL of methanol and 6 mL of ultra-water-pure. Samples were run through the cartridges in a continuous stream and then dried for 30 min. Elution of the analytes was done using 6 mL of acetonitrile and 6 mL of acetone, collected in round bottom flasks. The samples were taken to dry in a rotary evaporator and then reconstituted with 1 mL of acetonitrile and then subjected to ultrasound equipment.

Following the procedures mentioned above, 200 µL of the extracted sample was separated for the derivatization process for further analysis by gas chromatography. To carry out the derivatization process, the samples were first evaporated in 350 µL inserts in a 40 °C oven, after being completely evaporated, 50 µL of the derivatization agent (BSTFA + 1% TMCS) was added at a temperature of 60 °C for 30 min for the reaction. After this step, 150 µL of ethyl acetate was added for sample reconstitution.

Table 1. Compounds studied

Compound	Structures	Acronym	Class	^a log K _{ow}
Methylparaben		MeP	Preservative	1.96
Ethylparaben		EtP	Preservative	2.47
Propylparaben		PrP	Preservative	3.04
Butylparaben		BuP	Preservative	3.57
Benzylparaben		BzP	Preservative	3.59
Triclosan		TCS	Antibacterial	4.76

^alog K_{ow}: Octanol/water partition coefficient. Source: TOXNET, 2017¹¹.

2.3 Chromatographic Analysis

The compounds were analyzed on a 7890A GC-MS/MS (Agilent Technologies), equipped with a HP-5msi (30 m, 0.25 mm, 0.25 μm) silica capillary column coupled to a triple mass spectrometer quadrupole model 7000 with automatic sampler (PAL Sampler).

The chromatographic conditions applied were based on the method proposed by Mizukawa (2018)¹⁴. The injection was performed in Splitless mode. The temperature of the injection door was 280 °C and 2 μL of each sample were injected. A constant flow of 1 mL min⁻¹ of helium was used as carrier gas. The temperature of the oven was set at 100 °C (maintaining this temperature during 2 min), followed by an elevation of 15 °C min⁻¹ until 180 °C, 6 °C min⁻¹ until 270 °C, and 5 °C min⁻¹ until 310 °C, maintaining this temperature during 3 min. The resulting run time was 33.33 min. Temperatures of the transference

line and the ionization source were 280 °C. Nitrogen was used as a collision gas in a flux of 1.5 mL min⁻¹. Detection and quantification by MS/MS were performed in monitoring reaction mode.

2.4 Validation of the Chromatographic Method

In this study, the following parameters were evaluated: Linearity, sensitivity, limit of detection (LOD), limit of quantification (LOQ), accuracy and precision.

The methodology used to validate the analytical method was based on ANVISA Resolutions 475/02¹⁵ and 899/03¹⁶ and INMETRO's DOQ-CGCRE-008/03¹⁷.

2.4.1 Linearity and Sensitivity

An external standardization was used for the quantification of the compounds. Individual

standard stock solutions were prepared in methanol with a concentration of 1000 mg L⁻¹ and stored in a freezer. The mixed stock solutions were prepared diluting the standard individual stock solutions. Working solutions for the calibration solutions were prepared by direct dilution of the 10 mg L⁻¹ mix. Linearity was obtained by constructing an analytical curve with at least five concentrations, ranged between 0.05 – 1.0 mg L⁻¹. The sensitivity was expressed by the slope of the linear regression analytical curve and determined simultaneously with the linearity tests.

2.4.2 Limits of Detection and Quantification

LOD and LOQ were determined by Equations 1 and 2:

$$LOD = \frac{3 S_a}{IC} \quad (1)$$

$$LOQ = \frac{10 S_a}{IC} \quad (2)$$

where S_a is the estimate of the standard deviation of at least three whites and IC is the slope of the analytical curve.

2.4.3 Accuracy

Accuracy was assessed by ultrapure water recovery test. The value can be estimated by Equation 3:

$$\%recovery = \frac{x_{got}}{x_{added}} \times 100 \quad (3)$$

2.4.4 Precision

Precision was evaluated in terms of repeatability and intermediate precision by

calculating the absolute standard deviation and coefficient of variation for a minimum of six replicates.

3. Results and Discussion

The quality control parameters for the compounds analyzed are present in Table 1. The linearity of the method was measured by the linear regression coefficient and all the analytical curves had a minimum correlation coefficient equal to 0.99, so they are in accordance with what is recommended by ANVISA resolution 899/03¹⁶.

The sensitivity was expressed by the angle coefficient of the calibration curve that is, by the slope of the analytical curve and through it was possible to verify the tendencies of the sensitivity for each analyte. It is observed that propylparaben (PrP) was the compound that presented the highest sensitivity among the six personal care products analyzed by this analytical method. However, the sensitivity is not directly related to low detection limit values, but with a better precision in the quantification of values with similar concentrations¹⁸.

The lowest LOD and LOQ were found for benzylparaben (0.5 and 1.6 ng L⁻¹, respectively) and the highest for Methylparaben (14 and 48 ng L⁻¹). The limits of quantification were comparable to other studies that used the same type of detection and were satisfactory.

The accuracy of the proposed method was obtained from the analyte recovery test, which determines the recovery of the solid phase extraction by means of known concentrations of the compounds (0.1, 0.2, 0.4, 0.8 and 1.0 µg L⁻¹). Table 2 shows the mean values obtained in the recovery test of the compounds worked.

Table 2. Linear range, Analytical Curve, Correlation Coefficient (R^2), Sensitivity (slope), Method Limits of Detection and Quantification for Selected Compounds and Recovery Rates (R%).

Compound	Linear range (ng L ⁻¹)	Analytical curve	R^2	Slope	LOD (ng L ⁻¹)	LOQ (ng L ⁻¹)	Recovery Rates (%)
MeP	50 – 1000	$y = 174225x - 1617$	0.9956	1.7×10^5	14	48	56.8
EtP	50 – 1000	$y = 158440x - 3018$	0.9972	1.5×10^5	3.2	10	78.5
PrP	50 – 1000	$y = 203131x - 4872$	0.9981	2.0×10^5	0.9	3.2	111.4
BuP	50 – 1000	$y = 141603x - 3667$	0.9984	1.4×10^5	6.9	23	113.5
BzP	50 – 1000	$y = 126372x - 4773$	0.9943	1.2×10^5	0.5	1.6	117.9
TCS	50 – 1000	$y = 79002x - 2086$	0.9984	7.9×10^4	7.9	26	114

The method proved to be efficient for most of the compounds analyzed. With the exception of MeP and EtP, all other compounds recovered 100%. The low recovery rates of MeP and EtP can be justified by their low log K_{ow} values (1.96 and 2.47 respectively). According to the literature, the more polar the compounds ($\log K_{ow} \leq 3$), the efficiency of SPE is usually lower due to the solid phase used, octadecylsilane, that has a non-polar character¹⁹.

The results concerning repeatability and reproducibility are present, respectively, in Table 3. ANVISA (2003)¹⁶ does not admit, in precision analysis, coefficient of variance (CV) values higher than 5% for detection of drugs in pharmaceutical products, but for complex matrices this value does

not apply. In Resolution 475/02 of ANVISA (2002)¹⁴ it is stated that for more complex samples (blood, serum or plasma) CV values of up to 15% are allowed. In turn, INMETRO (2003)¹⁷ allows a CV of up to 20% for precision analysis of the method. In this work, the mean values of CV for analysis of repeatability and intermediate precision are within the established limit (15% - 20%), and therefore the method can be considered accurate for the analysis of the five PCPs. For EtP only, the reproducibility at the lowest concentration was above 15%. The best result among the PCPs studied was for the BzP, with average values 1.3% in intraday and 7.5% in between subsequent days.

Table 3. Coefficient of variance expressed as percentage of the intraday and between subsequent days assay of the compounds studied at three different concentrations (n=5)

Analitos	Repeatability				Reproducibility			
	0.05 mg L ⁻¹	0.2 mg L ⁻¹	1.0 mg L ⁻¹	Average	0.05 mg L ⁻¹	0.2 mg L ⁻¹	1.0 mg L ⁻¹	Average
MeP	2.8	1.1	4.6	2.8	10.3	5.1	10.8	8.7
EtP	1.4	2.5	2.0	2.0	18.0	2.9	6.1	9.0
PrP	2.7	6.0	4.9	4.5	14.9	10.5	8.6	11.3
BuP	0.9	1.2	4.4	2.2	15.7	7.0	3.6	8.8
BzP	1.2	1.4	1.2	1.3	7.7	5.6	9.2	7.5
TCS	1.9	1.7	0.5	1.4	10.4	9.6	9.8	9.9

3.1 Determination of parabens and triclosan in surface waters of the Palmital River

With the determination and evaluation of the main validation parameters, it was possible to apply the proposed chromatographic method in the analysis of PCPs in samples collected in the Palmital River.

In every sample analyzed in this research at least one of the parabens and triclosan were detected. Table 4 shows the concentration range found during the four sampling campaigns in the Palmital River. MeP and PrP were the parabens detected with the highest concentrations during the sampling campaign, reaching 0.40 and 0.22 $\mu\text{g L}^{-1}$. Differently from the parabens, the TCS was determined with greater frequency and in greater concentrations in the campaign of October of 2016, being that the greater concentration of this compound was of 0.19 $\mu\text{g L}^{-1}$.

From the results quoted above it was verified that the method was efficient to quantify the low concentrations detected in the Palmital River.

Table 4. Concentration range and average concentration of PCBs on the Palmital river.

Compound	Concentration ($\mu\text{g L}^{-1}$)	Average conc. ($\mu\text{g L}^{-1}$)
MeT	0.05 – 0.40	0.07
EtP	0.05	0.01
PrP	0.004 – 0.22	0.04
BuP	0.02 – 0.04	0.01
BzP	0.003 – 0.13	0.04
TCS	0.03 – 0.21	0.06

4. Conclusions

The results obtained in the validation of the chromatographic method were satisfactory and provided its reliability. All the parameters of merit worked had results according to the norms used for validation of analytical methods. The limits of detection and quantification were satisfactory and allowing the quantification of analytes at traces levels, in the ng L^{-1} range. With the application of the methodology, all the compounds studied were

quantified in the Palmital River, at least once at in trace levels.

The proposed methodology applies perfectly in the purpose initially established the detection of PCPs in surface waters and, finally, this method can be used as a basis for future monitoring of these compounds in environmental samples.

5. Acknowledgements

Financial support from CAPES Foundation, Ministry of Education of Brazil, for scholarship and PPGCTA - Post-Graduation Program in Environmental Science and Technology of UTFPR. Support CT-Infra 2010/ FINEP, Resources FNDCT, subproject NIPTA - Interdisciplinary Nucleus of Research in Environmental Technologies.

6. References

- [1] Brausch, J. M., Rand, G. M., A review of personal care products in the aquatic environment: environmental concentrations and toxicity, *Chemosphere* 82 (11) (2011) 1518-1532. <https://doi.org/10.1016/j.chemosphere.2010.11.018>.
- [2] Gottschall, N., Topp, E., Metcalfe, C., Edwards, M., Payne, M., Kleywegt, S., Lapen, D. R., Pharmaceutical and personal care products in groundwater, subsurface drainage, soil, and wheat grain, following a high single application of municipal biosolids to a field, *Chemosphere* 87 (2) (2012) 194-203. <https://doi.org/10.1016/j.chemosphere.2011.12.018>.
- [3] De García, S. O., García-Encina, P. A., Irusta-Mata, R., The potential ecotoxicological impact of pharmaceutical and personal care products on humans and freshwater, based on USEtox™ characterization factors. A Spanish case study of toxicity impact scores, *Sci. Total Environ.* 609 (2017) 429-445. <https://doi.org/10.1016/j.scitotenv.2017.07.148>.
- [4] Kolpin, D. W., Furlong, E. T., Meyer, M. T., Thurman, E. M., Zaugg, S. D., Barber, L. B., Buxton, H. T., Pharmaceuticals, hormones, and other organic wastewater contaminants in U.S. streams, 1999-2000: a national reconnaissance, *Environ. Sci. Technol.* 36 (6) (2002) 1202-11. <https://pubs.acs.org/doi/10.1021/es011055j>.
- [5] Halden, R. U., Paull, D. H., Co-occurrence of triclocarban and triclosan in U.S. water resources, *Environ. Sci. Technol.* 39 (6) (2005) 1420-1426. <https://pubs.acs.org/doi/abs/10.1021/es049071e>.
- [6] Mcavoy, D. C., Schatowitz, B., Jacob, M., Hauk, A., Eckhoff, W. S., Measurement of Triclosan In Wastewater Treatment Systems, *Environ. Toxicol. Chem.* 21 (7) (2002) 1323-1329. PMID:12109730.
- [7] Boberg, J., Taxvig, C., Christiansen, S., Hass, U., Possible endocrine disrupting effects of parabens and their metabolites, *Reprod. Toxicol.* 30 (2) (2010) 301-312. <https://doi.org/10.1016/j.reprotox.2010.03.011>.
- [8] Caliman, F. A., Gavrilesco, M., Pharmaceuticals, personal care products and endocrine disrupting agents in the environment—a review, *Clean* 37 (2009) 277-303. <https://doi.org/10.1002/clen.200900038>.
- [9] Piao, C., Chen, L., Wang, Y., A review of the extraction and chromatographic determination methods for the analysis of parabens, *Journal of Chromatography B.* 969 (2014) 139-148. <https://doi.org/10.1016/j.jchromb.2014.08.015>.
- [10] Pérez, S., Barceló, D., Application of advanced MS techniques to analysis and identification of human and microbial metabolites of pharmaceuticals in the aquatic environment, *Trends in Analytical Chemistry* 26 (6) (2007) 494-514. <https://doi.org/10.1016/j.trac.2007.05.004>.
- [11] Sui, Q., Huang, J., Deng, S., Yu, G., Fan, Q., Occurrence and removal of pharmaceuticals, caffeine and DEET in wastewater treatment plants of Beijing, China, *Water Res.* 44 (2) (2010) 417-426. <https://doi.org/10.1016/j.watres.2009.07.010>.
- [12] Scognamiglio, V., Antonacci, A., Patrolecco, L., Lambrea, M. D., Litescu, S. C., Ghuge, S. A., Rea, G., Analytical tools monitoring endocrine disrupting chemicals, *Trends in Analytical Chemistry* 80 (2016) 555-567. <https://doi.org/10.1016/j.trac.2016.04.014>.

[13] Toxnet, toxnet.nlm.nih.gov. Accessed in July 2017.

[14] Ide, A. H., Cardoso, F. D., Marques dos Santos, M., Kramer, R. D., Rodrigues de Azevedo, J. C., Mizukawa, A., Utilização da Cafeína como Indicador de Contaminação por Esgotos Domésticos na Bacia do Alto Iguaçu, *Rev. Bra. Recur. Hídricos* 18 (2) (2013) 201–211.

[15] Mizukawa, A., Reichert, G., Filipe, T. C., Brehm, F. D. A., Rodrigues de Azevedo, J. C., Occurrence and Risk Assessment of Personal Care Products in Subtropical Urban Rivers, *Environmental Engineering Science* 35 (11) (2018). <https://doi.org/10.1089/ees.2018.0066>.

[16] ANVISA - Agência Nacional de Vigilância Sanitária; Resolução - RE nº 475, de 19 de março de 2002.

[17] ANVISA - Agência Nacional de Vigilância Sanitária; Resolução - RE nº 899, de 29 de maio de 2003.

[18] INMETRO - Instituto Nacional de Metrologia, Normalização e Qualidade Industrial; Orientações sobre validação de métodos de ensaios químicos; DOQ-CGCRE-008, março de 2003.

[19] Kramer, R. D., Mizukawa, A., Ide, A. H., Marcante, L. O., Determinação de anti-inflamatórios na água e sedimento e suas relações com a qualidade da água na bacia do Alto Iguaçu, Curitiba-PR, *Rev. Bra. Recur. Hídricos* 20 (2015) 657–667.

Determination of the concentration of Ce, La, Sm and Eu in a phosphogypsum stack, in Imbituba city, Santa Catarina, Brazil

Renata Coura Borges¹⁺, Letícia Mombrini Marques², Cláudio Fernando Mahler¹, Alfredo Victor Bellido Bernedo³

¹ Federal University of Rio de Janeiro (UFRJ), 2030-101 Horácio Macedo St, Rio de Janeiro, Rio de Janeiro, Brazil

² Federal Institute of Education, Science and Technology of Rio de Janeiro (IFRJ), Washington Luís Hw, Niterói, Rio de Janeiro, Brazil

³ Fluminense Federal University (UFF), 9 Miguel de Frias St, Niterói, Rio de Janeiro, Brazil

+ Corresponding author: Renata Coura Borges, e-mail address: renatacouraborges@hotmail.com

ARTICLE INFO

Article history:

Received: February 05, 2018

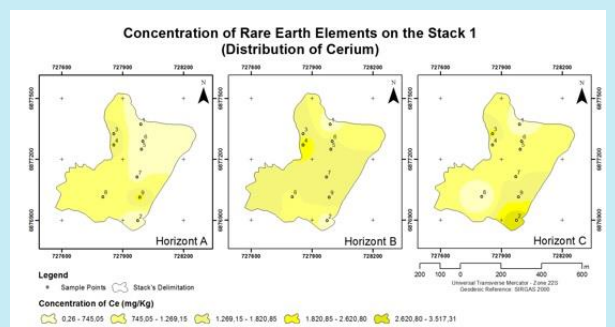
Accepted: September 07, 2018

Published: October 07, 2018

Keywords:

1. phosphogypsum;
2. geoprocessing;
3. rare-earth elements.

ABSTRACT: Phosphate fertilizer industry produces phosphoric acid from phosphate rocks, and as a byproduct, it produces phosphogypsum, also known as agricultural gypsum. This material was stocked in open-air stacks near the producing units. In order to determine levels of rare-earth elements in phosphogypsum stacks, located in Imbituba, Brazil, samples of 2000 grams of phosphogypsum were collected in nine different points in stack 1. The concentration of rare-earth elements was determined through neutron activation analysis and results indicate significant values of rare-earth elements in the phosphogypsum from Imbituba, when compared to the values of the Earth's crust.



1. Introduction

Phosphogypsum is a byproduct of phosphoric acid industry and it comes from acid leaching of phosphate rock with water and concentrated sulfuric acid. Phosphogypsum is a calcium sulfate dehydrate, which physical and chemical characteristics are equal to natural gypsum. Although phosphogypsum is mostly composed of calcium sulfate dehydrate, impurities from the original phosphate rock can be identified in high levels. These impurities are redistributed between the phosphoric acid and the phosphogypsum, during the manufacture. The insoluble impurities (or solubilized in the acid medium) consist of chemical elements, such as metals, rare-earth elements, fluorides and radionuclides¹.

Rare-earth elements can enter into human organism by ingesting contaminated food and

inhaling particles in suspension. Most of rare-earth elements, which are ingested, were excrete, although a short part can enter the bloodstream and accumulate in different parts of human body per ion exchange processes².

An extensive volume of phosphogypsum generated annually by phosphoric acid production industries in world has been receiving attention of radiological and environmental protection agencies. In the Brazilian state of Santa Catarina, there is a stack of the material, located in the city of Imbituba, south of the state capital, Florianópolis. This material is currently commercialized and applied in apple and soybean crops. Some studies with Brazilian phosphogypsum have already been performed. However, there are no studies on phosphogypsum from this Brazilian State, and specially, on its toxicity by rare-earth elements.

This work aimed to quantify the presence of rare-earth elements (Sm, La, Ce, Eu) in phosphogypsum of Imbituba - Santa Catarina.

2. Materials and methods

2.1 Study site

Georeferenced samples of the PG (phosphogypsum) studied were collected in nine

points in PG stack 1 (Figure 1), in the city of Imbituba, southern coast of Brazilian state of Santa Catarina ($28^{\circ} 13' 17''$ S and $48^{\circ} 38' 21''$ W). In addition, samples were collected in the Referenced Area (AR), with the purpose of comparison related to the chemical composition of the local soil without human interference (background value).

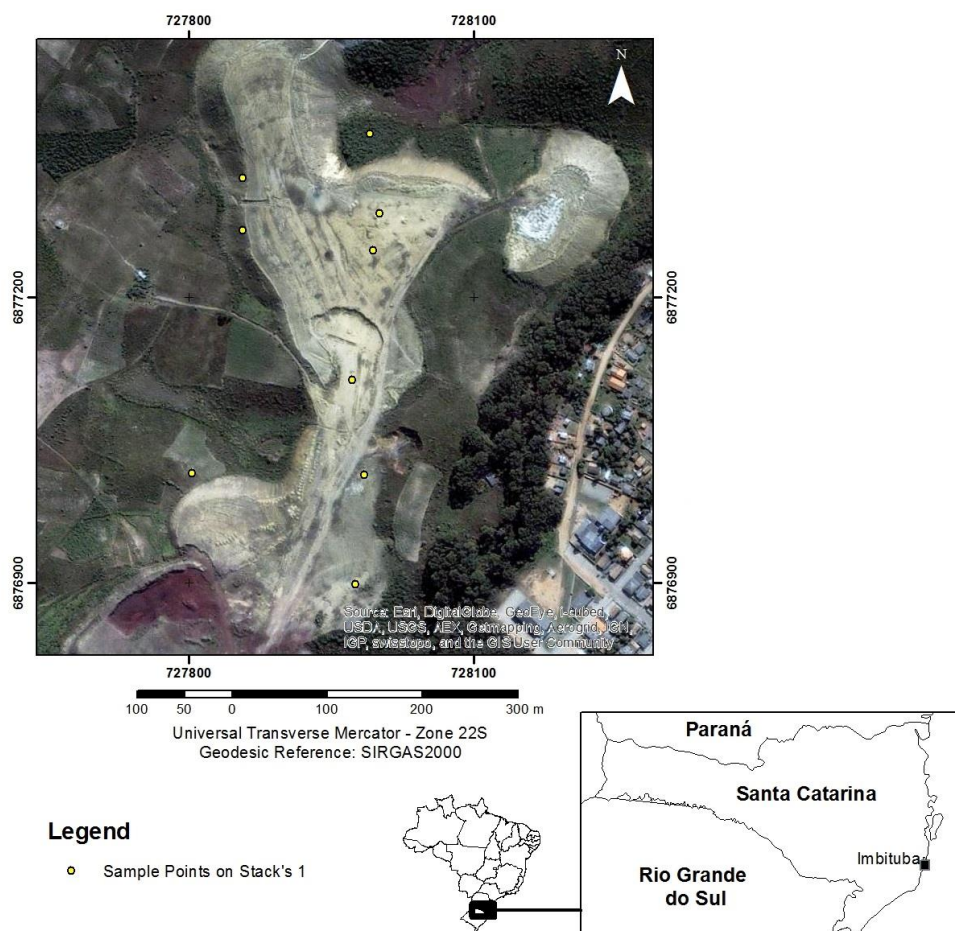


Figure 1. Georeferenced samples of PG.

2.2 Sample collection and preparation

Sampling procedures were managed in accordance to the Brazilian Association of Technical Standards (ABNT)³. The samples were collected in Engessul/Imbituba-SC, in May of 2008. The sampling procedures consisted on sample extraction, at different depths: 0 – 0.20 m (horizon A), 0.20 – 1 m (horizon B) and 1 – 2 m (horizon C) with the purpose of evaluation of the distribution of chemical elements according to the stack depth. The samples composed of 2000 grams

of phosphogypsum in each depth were conditioned in plastic bags previously identified and transported to the laboratory for posterior analysis. The soil samples followed the same procedures applied to the phosphogypsum.

All PG and soil samples were identified, grounded with a 2 mm mesh sieve at ambient temperature, to achieve a fine powder, and finally oven dried to constant weight.

2.3 Determination of rare-earth elements in the samples

To determine the levels of rare-earth elements in phosphogypsum and soil, the neutron activation analysis method was applied. Powder samples were homogenized in an agate mortar, individually. Around 200 mg of each sample was packed in polyethylene capsules using a four-decimal-place-graduated analytical balance. Capsules were sealed using a soldering tool with a graphite tip. Samples were irradiated for four hours in a thermal neutron flux of 10^{13} n cm⁻² s⁻¹ in the IEA-R1 nuclear reactor at Institute of Nuclear and Energetic Research (IPEN), São Paulo city, Brazil. In addition, “control” polyethylene capsules were also irradiated.

The standard used was the San Joaquin Soil (NIST 2709), that was prepared in the same way as samples with the view to guarantee the same geometries. To assess the data consistence and to guarantee the accuracy and reproducibility of the analysis, to each set of ten samples, one “control” sample and three samples of reference materials were analyzed.

The elements determined by this technique were Sm, Eu, La and Ce.

2.4 Statistical Analysis

Owing to the complexity and variability normally observed in environmental studies, it is common the use of multivariate statistical methods to differentiate and identify natural levels of heavy metals from anthropogenic contamination. With the view to verify parameters that contribute with the characterization and how they were related with the methods used, cluster analysis was performed using STATISTICA 7 software (StatSoft Inc.).

3. Results and discussion

3.1 Concentration of rare-earth elements

The REE (rare-earth elements) in phosphogypsum derive by its raw material (phosphate rocks). There were two kinds of phosphate rocks: the sedimentary and igneous rock. The ore matrix used in the acid production process is the source of REE in the phosphogypsum. Phosphogypsum generated in Imbituba-SC was composed by phosphate rocks from igneous origins. Stack 1 was formed by igneous phosphate ores from Araxá – MG.

Table 1 presents rare-earth concentration values found in phosphogypsum analyzed in present study.

Table 1. Concentration (mean \pm standard deviation mg kg⁻¹) of REE from phosphogypsum in samples from other sources.

Element	Russia ⁴	Brazil ⁵	Brazil ⁶	Brazil ⁷	Stack 1
Ce	1600	2574	956	1730	1233 \pm 326
La	1050	1300	1017	973	27 \pm 4
Eu	30.4	36	26	29	36 \pm 3
Sm	76	149	123	85	70 \pm 12

Results showed that for Ce there were no large variations in the concentration, whereas La has a lower concentration in relation to those found by other authors. Eu and Sm present values close to those found in phosphogypsum from other regions. The summation (Σ) of the total concentration of the REE (Ce, La, Eu and Sm) in the studied phosphogypsum was 1366.3 mg kg⁻¹.

Figures 2, 3, 4 and 5 show the distribution of REE in relation to the depth in phosphogypsum of Imbituba.

Figure 2 presents Cerium (Ce) results. In the Earth's crust, the mean concentration of Ce is 66 mg kg⁻¹, and in Chinese soils, the average concentration found in eight different types of soils was 86 mg kg⁻¹⁸. In Dutch soils, the maximum allowable concentration for Ce is 53 mg kg⁻¹⁹.

There are no established guidelines values for this element in Brazil. Although, in this study,

stack 1 has Ce values much higher than the allowed.

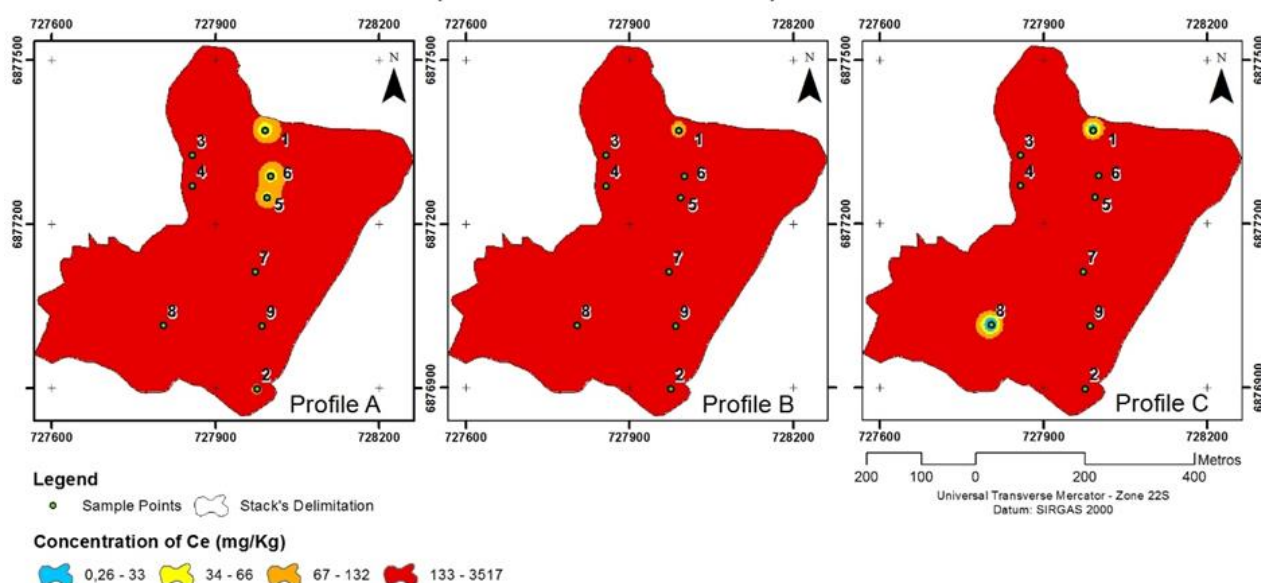


Figure 2. Distribution of Cerium on the stack 1.

According to Lapido-Loureiro *et al.* (2008)¹⁰, apatite, along with its varieties, form a relevant group of minerals. The Ca^{2+} can be replaced, principally, by rare-earth element light in igneous apatite and rare-earth element heavy in sedimentary origin. The results confirm this data, since stack 1 was formed by igneous rocks that were enriched with Cerium.

Comparing the values of Ce in igneous phosphate ores¹¹, the concentration in stack 1 was in the range for the apatite in Norway (494.4–5352.9 mg kg^{-1}), which confirms, again, the high concentration of REE in igneous rocks.

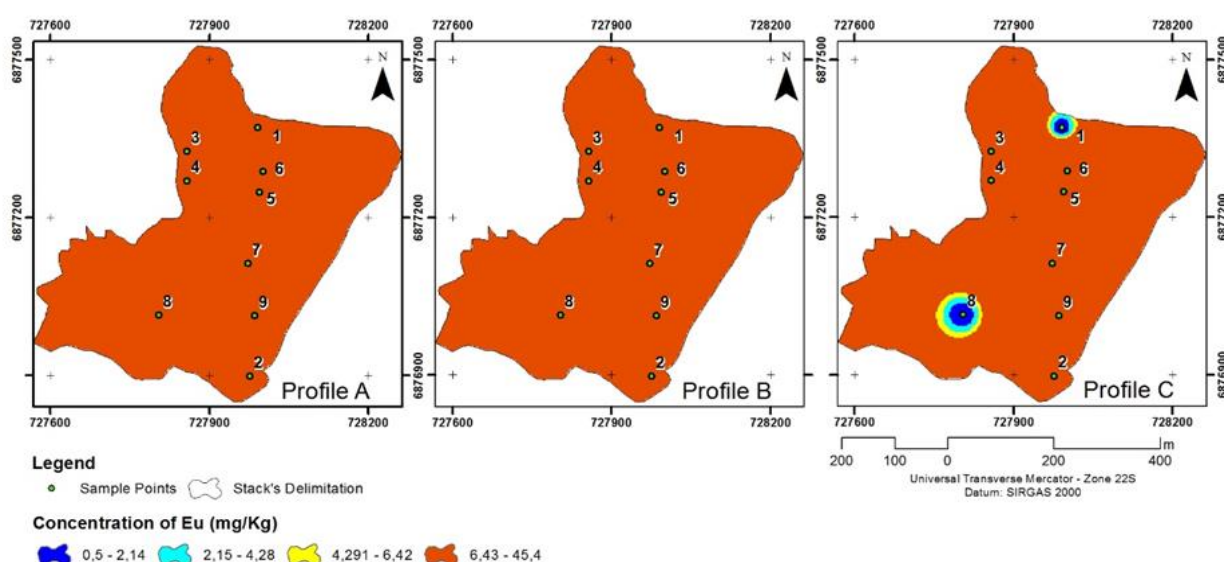


Figure 3. Distribution of Europium on the stack 1.

Figure 3 presents results for Europium (Eu). Eu is an element not found in nature as a free element and it is difficult its separation. The oxidation states

are +3 and +2 and Eu was found in ores containing small amounts of all REE. In the Earth's crust, the mean concentration of Europium is about 2.14 mg

kg^{-1} ¹². The average value obtained in stack 1 was 35 mg kg^{-1} , higher than the determined for the crust and soil, but still in the concentration range found in igneous phosphate rocks $21.5 - 73.7$ ¹¹.

Evaluating the Eu concentration, according to the depths, it is possible to observe that the values

decreased as the depth increased; that is, the horizons B and C presented lower concentration of the element.

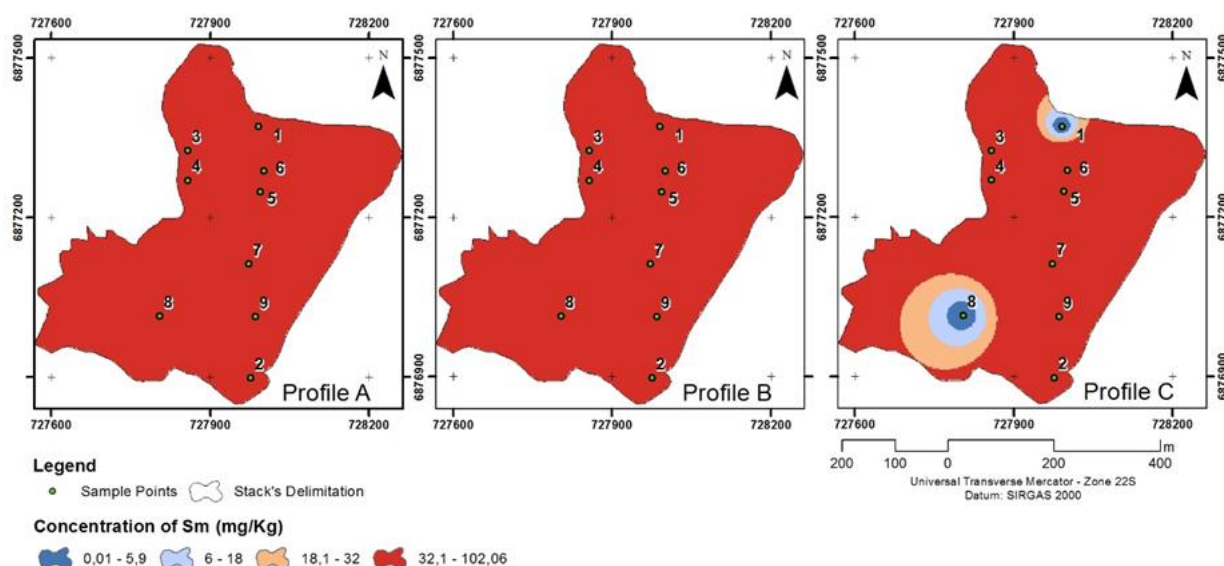


Figure 4. Distribution of Samarium on the stack 1.

Figure 4 presents results for Samarium (Sm). In stack 1, the average concentration of Sm found in phosphogypsum was 70 mg kg^{-1} , less than mentioned by Ihlen *et al.* (2014)¹¹, that found a concentration in the range of $86.3 - 323.3 \text{ mg kg}^{-1}$ in igneous phosphate rocks. Presumably, this is

related to the redistribution of Sm that has undergone chemical processing of phosphate rock.

Noticing the concentration over the depth: surface samples showed the highest concentration of this element and samples from the third depth, the lowest level.

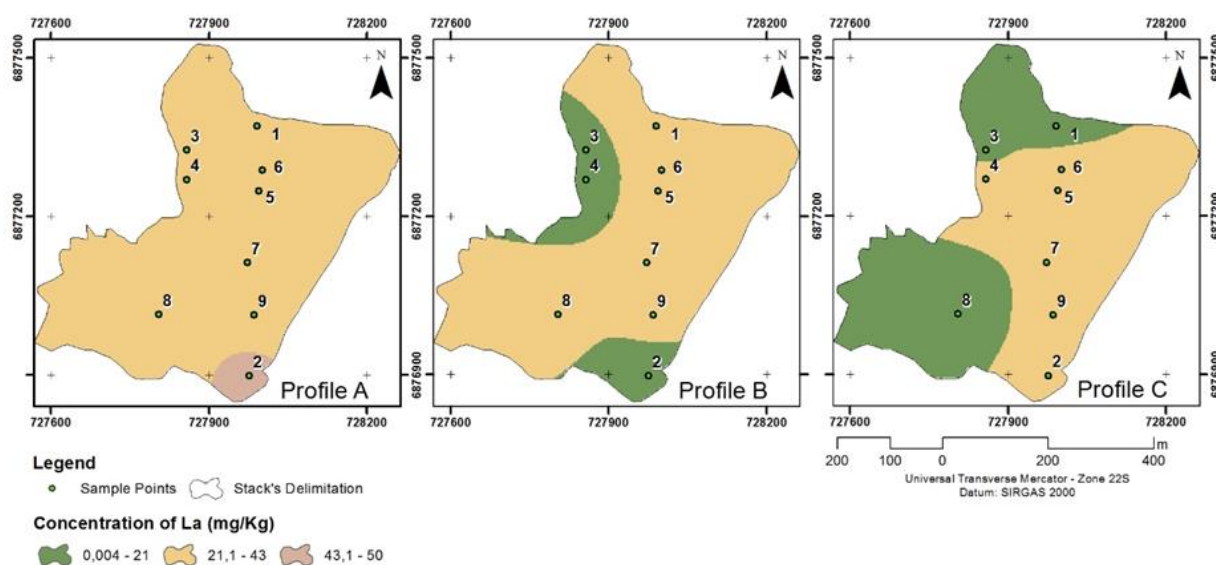


Figure 5. Distribution of Lanthanum on the stack 1.

Figure 5 shows results for Lanthanum (La). In the Earth's crust, the mean value found was 43 mg kg⁻¹¹³. Concentration found to La, in samples from stack 1, were considered intermediate, when compared to the values determined for igneous rocks and below, when compared to the global average. Furthermore, few samples of phosphogypsum collected in the second and third depth of the stack 1 showed the maximum concentration for La.

It was observed that La, Eu and Sm underwent little variation with depth, and Ce, in some points, presented a great variation; this is because REE in phosphogypsum samples were associated to the formation of carbonates, fluorides, sulfates and phosphates of these elements⁸.

The experimental results and the certified values are in Table 2.

Table 2. Concentration (mean \pm standard deviation mg kg⁻¹) of REE from different literatures, reference area and standard certificate

Element	Earth Crust ⁸	Referenced Area	San Joaquin Soil (Experimental Values)	San Joaquin Soil (Certified Values)	Sandy soil ⁷	Soil in Japan ¹⁴
Ce	66	0.14 \pm 0.01	0.044 \pm 0.001	0.042 \pm 0.001	21 \pm 1	33
La	35	14.5 \pm 0.3	0.026 \pm 0.001	0.023 \pm 0.001	3.0 \pm 0.3	15
Eu	2.1	5.1 \pm 0.3	0.011 \pm 0.001	0.009 \pm 0.001	<0.04	0.8
Sm	7	4.1 \pm 0.2	0.038 \pm 0.001	0.038 \pm 0.001	0.39 \pm 0.02	3.4

The results obtained by the evaluation of the influence of the phosphogypsum stacks to the surrounding soil (RA) were presented in Table 2 with other results from the literature.

The REE concentration results in RA soil samples were inferior to the values found in other researches, for the Earth's crust, with exception of element Eu, which presented higher concentrations.

In contrast, the RA soil showed heavy REE enrichment, indicating that the stacks have changed in some way the concentration of the elements in the soil under its influence.

Comparing the RA results to the soils found in other researches, it is possible to observe that the

Ce concentration was lower than in the soils from Japan and sandy soils. The La and Sm concentrations, however, were close to the values found in Japanese soils and higher than Brazilian sandy soils. On the other hand, the Eu had its concentration higher in the RA than in the other researches, which indicate that there was an increase of the element on this area.

3.2 Statistical Analysis – Cluster

Figure 6 shows the result of Cluster analysis using the software STATISTICA 7 (StatSoft Inc.).

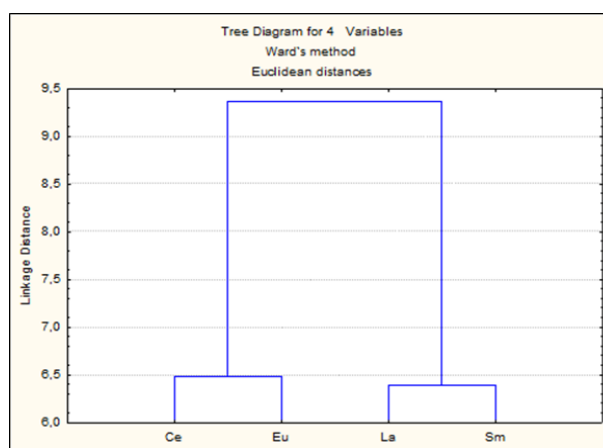


Figure 6. Cluster analysis.

It is possible to observe that there is the formation of two large similarity groups: first, composed by Ce and Eu, which presented much higher concentrations in the phosphogypsum than in the Earth's crust; and the second, composed by La and Sm, whose concentrations were closer to the results obtained for the Earth's crust.

4. Conclusions

The result obtained (Σ REE the order of 1366.3 mg kg⁻¹) indicated that the phosphogypsum produced in Imbituba has a high concentration of REE when compared with background values found in environmental samples. High concentration of rare-earths in phosphogypsum suggests that these elements may contaminate animals, plants, rivers, lakes and consequently humans during the ingestion of food grown on soils treated with this phosphogypsum.

Results showed a high concentration of Ce and Eu and a concentration below the global average of La when compared to igneous rocks from other regions. However, Eu and Sm presented values close to those found in phosphogypsum of other regions. This is due to the origin of matrix rock used in the processing, which may vary the concentration of REE in phosphogypsum.

5. Acknowledgments

The authors would like to acknowledge the Conselho Nacional de Desenvolvimento Científico e Tecnológico (CNPq) and Coordenação de Aperfeiçoamento de Pessoal de Nível Superior (CAPES) for the scholarship and financial support.

6. References

- [1] Associação brasileira de normas técnicas. NBR 10006: Solubilização de resíduos, Rio de Janeiro, 1987.
- [2] Fernandes, H. M., Rio, A. P. M., Franklin, M. R., Impactos Radiológicos da Indústria do Fosfato, Série Estudos & Documentos CETEM/MCT 56 (2004).
- [3] Koeberl, O., Bayer, P. M., Concentrations of rare-earth elements in human brain tissue and kidney stones determined by neutron activation analysis, *Journal of Alloys Compounds*, 180 (1998) 63 - 70.
- [4] Gorbunov, A. V., Frontasyeva, M. V., Gundorina, S. F., Onischenko, T. L., Maksiuta, B. B., Chen Sen Pal, Effect of agricultural use of phosphogypsum on trace elements in soils and vegetation, *Science of the Total Environment* 122 (3) (1992) 337-346. [https://doi.org/10.1016/0048-9697\(92\)90051-S](https://doi.org/10.1016/0048-9697(92)90051-S).
- [5] Santos, A. J. G., Mazzilli, B. P., Fávoro, D. I. T., Silva, P. S. C., Partitioning of radionuclides and trace elements in phosphogypsum and its source materials based on sequential extraction methods, *Journal of Environmental Radioactivity* 87 (2006) 52-61. <https://doi.org/10.1016/j.jenvrad.2005.10.008>.
- [6] Lebourlegat, F. M., Disponibilidade de Metais em Amostras de Fosfógeno e Fertilizantes Fosfatados Utilizados na Agricultura, 2010, 88f. Dissertação (Mestrado) – Instituto de Pesquisas Energéticas e Nucleares, São Paulo, 2010.
- [7] Oliveira, K. A. P., Fator de Transferência de Elementos Terras Raras em Solos Tropicais Tratados com Fosfógeno, 2012, 133f. Tese (Doutorado) – Saneamento, Meio Ambiente e Recursos Hídricos, UFMG, Belo Horizonte, 2012.
- [8] Tyler, G., Rare-earth elements in soil and plant system – A review, *Plant and Soil*. 267 (2004) 191-206.
- [9] Sneller, F. E. C., Kalf, D. F., Weltje, L., Wezel Van, A. P., Maximum Permissible Concentrations and Negligible Concentrations for Rare Earth Elements (REEs). IVM-National Institute for Public Health and the Environment, report 601501011: The Netherlands, 2000.
- [10] Lapido-Loureiro, F. E., Fertilizantes e sustentabilidade: o fósforo na agricultura brasileira, Série de Estudos e Documentos, CETEM, 2008.
- [11] Ihlen, P.M., Schiellerup, H., Gautneb, H., Skar, O., Characterization of apatite resources in Norway and their REE potential - A review, *Ore Geology Reviews* 58 (2013) 126-147. <https://doi.org/10.1016/j.oregeorev.2013.11.003>.

[12] Fortescue, J. A. C., Landscape geochemistry: retrospect and prospect – 1990, *Applied Geochemistry*, 7 (1992) 1-53.

[13] Kabata-Pendias, A., Pendias, H., Trace elements in soils and plants, Boca Raton, 2nd ed., 1992.

[14] Uchida, S., Tagami, K., Hirai, I., Soil-to-plant transfer factors of stable elements and naturally occurring radionuclides (1) Upland field crops collected in Japan, *Journal of Nuclear Science and Technology* 44 (4) (2007) 628-640. <https://doi.org/10.1080/18811248.2007.9711851>.

Biosorption of 5G blue reactive dye using waste rice husk

Ismael Laurindo Costa Junior¹, Leandro Finger², Poliana Paula Quitaiski², Samuel Mathias Neitzke¹, Josue Victor Besen¹, Maike Krug Correa¹, Juliana Bortoli Rodrigues Mees²

¹ Federal Technological University of Paraná, Campus Medianeira, Department of Chemistry, 4232 Brasil Av, Medianeira, Paraná, Brazil

² Federal Technological University of Paraná, Campus Medianeira, Department of Biological and Environmental Sciences, 4232 Brasil Av, Medianeira, Paraná, Brazil

* Corresponding author: Ismael Laurindo Costa Junior, e-mail address: ismael@utfpr.edu.br

ARTICLE INFO

Article history:

Received: December 22, 2017

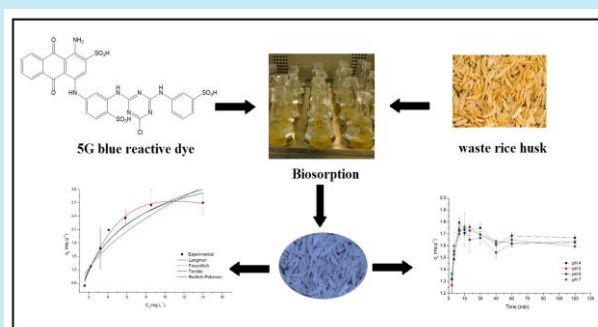
Accepted: October 06, 2018

Published: October 07, 2018

Keywords:

1. biosorbent
2. adsorption isotherms
3. 5G Reactive Dye
4. waste rice husk

ABSTRACT: In this study, the biosorption was used on the removal of 5G blue dye using rice husk residue. The influence of temperature and pH on the biomass pretreated with H₃PO₄ and NH₄Cl was evaluated on the sorption capacity. The tests were conducted in batch with previous determination of point of zero charge (PZC). Analytical measurements were performed by UV-VIS spectroscopy. A major influence of pH and temperature on the biosorption capacity of the dye was observed. The highest removal was obtained for the condition of pH 4 and temperature of 50 °C. The time for the biomass-dye system to reach equilibrium was around 45 min. Pseudo-first order kinetic model adequately represented experimental data and had a good correlation coefficient. In the equilibrium study, Langmuir isotherm best fitted the experimental data, with a maximum biosorption capacity of 3.84 mg g⁻¹. The use of rice husk as a biosorbent for the removal of reactive blue 5G dye can be considered promising for the abundance of this residue and the observed sorption capacity.



1. Introduction

In the industrial sector, several projects have been highlighted by the polluting potential, especially by the considerable amounts of residues rich in diverse types of substances highly harmful to water, air and soil. In this category, the textile industries are included as generators of environmental impacts and emitters of waste typically composed of the inputs used in its process, among which dyes, such as reactive blue dye 5G used on a large scale in the production of denim^{1,2}.

Reactive dyes have been used on a growing scale by the textile industries due to their reactivity with fibers and color stability. The reactive dye

molecule can be defined by the following structural systems: a chromophore system, responsible for the color phenomenon; a sulfonate group, responsible for the solubility and anionic character of the dye; and one or more reactive groups, which may form a covalent bond with the cellulose fibers by nucleophilic addition or substitution reaction³.

The increase of complexity and difficulty for the treatment of industrial effluents has led to the search of new methodologies for the removal of these wastes. The availability of innovative technologies and costs compatible with the need to reduce the environmental liabilities produced by industrial effluents is a fundamental task with repercussions in the short and medium term. As a measure to minimize the impacts caused by the

discharge of effluents rich in specific pollutants such as dyes, companies have the option of using tertiary treatments, mainly physical and chemical. Currently, due to the cost and operational complexity, these systems have been neglected by alternative systems or the use of biomass through the processes of bioaccumulation and biosorption^{4,5}.

Biosorption is a passive process where the capture is carried out by inactive (dead) biomass. The capture of the contaminants by biomass occurs through physical-chemical interactions between the ions and the functional groups present on the biomass surface⁶.

A variety of biosorbents have been investigated such as banana peel, chitosan, orange peel, aquatic plants, cotton fibers, wood sawdust, sugarcane bagasse, corn cob, babassu coconut, among others^{7,8}. Aiming for efficiency, kinetic and equilibrium studies are required to better understand the mechanisms involved. The pseudo-first and pseudo-second order models are commonly applied for kinetic evaluation. For the biosorption equilibrium, isotherms are used to describe the experimental data accurately within a set of imposed conditions⁹. The commonly used models are Langmuir, Freundlich and Henry^{10,11}.

Rice husk is a lignocellulosic compound formed, basically, by: i) cellulose (35%), a semi-crystalline polymer of anhydrocellulose, the units of which are interconnected via β -1 \rightarrow 4 bonds; (ii) hemicellulose (13.1%), a heterogeneous polymer composed of the combination of three hexoses: β -D-glucose, β -D-mannose and β -D-galactose, three pentoses: β -D-xylopyranose, β -D-arabinopyranose and β -D-galactouronic acid; and (iii) lignin (13.27%), an amorphous aromatic polymer (methoxy-phenols forming a resin species in plants), consisting of two types of basic units: guaiac and syringyl¹². This biomass is insoluble in water, has good chemical stability, high mechanical strength and has several functional groups in its structure such as COOH, -OH, SiOH, CH, C=O, C=C, CH₂, CH₃, CO, Si-O-Si, Si-H, -O-CH₃, and therefore has potential to be a good adsorbent material^{13,14}.

Biosorbents prepared with rice husk have been used in the adsorption of heavy metals, dyes and other organic compounds due to the large renewable production and the low cost for these adsorbents¹⁵⁻¹⁸. Previous researches reveal that rice husk can be used for removing ionic dyes from aqueous solutions and presented promising results.

This biomass presents high adsorption capacity, which is significantly increased when chemically modified¹⁹⁻²¹.

This study investigated the removal of 5G blue reactive dye by means of biosorption using the rice husk residue as a biosorbent. Kinetic and equilibrium studies were performed to evaluate this biomass as a low-cost alternative, when compared to traditional physicochemical systems.

2. Materials and methods

2.1 Reagents, solutions and analytical determinations

All reagents used in this work were analytical grade, phosphoric acid 85% (Merck), sodium hydroxide 97% (Merck), hydrochloric acid 37% (Merck), ammonium chloride P.A. (VETEC) and sodium chloride P.A. (VETEC). Reactive dye 5G (TEXPAL) of commercial nature was used in powder form.

Solutions were prepared at the concentration of 1.0 mol L⁻¹ for biomass treatments and for determination of the point of zero charge (PZC). From a stock solution of the 1000 mg L⁻¹ dye and distilled water, working solutions were prepared with 20 mg L⁻¹ used in the adsorption experiments.

The determination of the concentration of dye in the tests occurred by external calibration. For this, a six-point analytical curve was obtained using stock solution in the range from 0 to 50 mg L⁻¹. Measurements were performed using a UV-VIS spectrophotometer (Perkin Elmer Lambda 45) at 589 nm. The pH measurements were performed in bench potentiometer (Hanna 21).

2.2 Preparation of the biosorbent

Approximately 1.5 kg of rice husk were cleaned with distilled water by immersion for 24 h. Subsequently, the material was drained and oven dried (Quimis) for 24 h at 60 °C. Subsequently the biomass was ground in a knife mill and divided into three equal portions. One of them was reserved as experimental blank. To evaluate the influence of chemical pretreatments, one of the portions of the dried rice husk was immersed in 1.0 mol L⁻¹ H₃PO₄, and the other was immersed in 1.0 mol L⁻¹ NH₄Cl for 24 h. After rinsing again with distilled water, they were again dried in an oven and packed in sealed containers.

2.3 Point of zero charge (PZC)

The adsorption processes are strongly dependent on the pH, which affects the surface charge of the adsorbent, the degree of ionization and the adsorbate species. The pH_{PCZ} allows to predict the charge on the surface of the adsorbent as a function of pH. For the determination of the pH_{PCZ} , samples composed of 0.5 g of rice husk were placed in Erlenmeyer flasks with 50 mL of NaCl 0.1 mol L⁻¹ solution and adjusted pH 2 to 12 with NaOH and HCl 0.1 mol L⁻¹. The plastic film sealed bottles were kept under constant stirring (120 rpm) in a shaker incubator (Lactea brand, model LAC-2000) at 25 °C. The pH was measured at intervals of 1 h until constant values were obtained. Stirring was continued for 24 h to ensure equilibrium of the solutions. The values were presented as a plot of $\Delta pH \times$ initial pH, and the PCZ value defined as the one that intercepts the x-axis ($\Delta pH = 0$)²².

2.4 Biosorption Study

For the pH effect evaluation, two values above and two below of the PZC were chosen. To study the temperature, tests were performed at 40 and 50 °C, in addition to the ambient temperature (25 °C). The assays were carried out in duplicate in a 125 mL Erlenmeyer flask, kept under shaking at 120 rpm in a shaker incubator. 0.5 g of biosorbent and 50 mL of dye solution (20.0 mg L⁻¹) were added to each flask for kinetic test and at concentrations of 1.0, 5.0, 10.0, 15.0, 20.0, 25.0, 30.0, 35.0 and 40.0 mg L⁻¹ for isotherm equilibrium test. After 4 h, the biosorbent was removed by filtration and the dye concentrations were measured by using the spectrophotometer mentioned before.

The concentration of the dye in the adsorbent (q_e), in mg g⁻¹, was calculated by Equation 1.

$$q_e = V \cdot \frac{(C_0 - C_e)}{m} \quad (1)$$

where V is the volume of the solution (L), C_0 is the initial concentration of the solution (mg L⁻¹), C_e is the concentration of the final test solution (mg L⁻¹). The dye concentration at equilibrium (q_e) was determined by the inspection of the graph time $q_e(t)$ versus (t), at the instant the removal was constant.

The equilibrium kinetic data were fitted to the

pseudo-first order models (Eq. 2), pseudo-second order (Eq. 3) and the intraparticle diffusion model derived from Fick's law assuming that diffusion of the liquid film surrounding the adsorbent is negligible and intraparticle diffusion is the rate-determining step of the adsorption process (Eq. 4)²³⁻²⁵.

$$q(t) = q_e(1 - e^{-k_1 t}) \quad (2)$$

$$q(t) = \frac{(q_e)^2 k_2 t}{(q_e k_2 t) + 1} \quad (3)$$

$$q(t) = k_3 t^{\frac{1}{2}} + C \quad (4)$$

where q_e and $q(t)$ are the equilibrium adsorption and the adsorption capacity at the time t , respectively, in mg g⁻¹; t is the time in min; C suggests the thickness of the boundary layer effect (mg g⁻¹); k_1 (min⁻¹), k_2 (g mg⁻¹ min⁻¹) and k_3 (g mg⁻¹ min^{-1/2}) are the constants corresponding to the pseudo-first, pseudo second order and intraparticle diffusion models, respectively.

To describe the adsorption equilibrium, the adsorption isotherms models were adjusted to experimental data. Langmuir model hypothesizes that adsorption occurs in a monolayer manner and that all active sites are evenly distributed on the adsorbent and are available at the same energy "cost". These facts are important for the description of the interaction adsorbent-adsorbate (Eq. 5).

$$q_e = \frac{q_m \cdot b \cdot C_e}{1 + b \cdot C_e} \quad (5)$$

where q_m is the adsorption capacity of the studied material (mg g⁻¹); and b is the constant that measures the adsorbent-adsorbate affinity related to adsorption-free energy^{26, 27}.

The Freundlich model (Eq. 6) considers the heterogeneous solid and the exponential distribution to characterize the diverse types of adsorption sites, with different adsorptive energies²⁸.

$$q_e = k_L \cdot C_e^{1/n} \quad (6)$$

where k_L and n are empirical constants²⁹ and can be related to the changes in the adsorbed concentration with the changes in the solute concentration.

The Temkin model (Eq. 7) considers the effects

of the indirect interactions between the adsorbate molecules and the decrease of the heat of adsorption with the increase of the rate of removal³⁰.

$$q_e = B \cdot \ln k_T C_e \quad (7)$$

where B is the Temkin constant relating the heat of adsorption to the total number of sites (mg g^{-1}) and k_T is the Temkin constant (L mg^{-1}).

The Redlich-Peterson model (Eq. 8) is used to represent equilibrium of adsorption over a wide range of concentrations and may be applied in homogeneous and heterogeneous systems, due to its versatility³¹.

$$q_e = \frac{k_R C_e}{1 + a_R C_e^\beta} \quad (8)$$

where k_R and a_R are the Redlich-Peterson constants (L mg^{-1}) and β is the exponent with values from 0 to 1. The parameters of the models were obtained from non-linear regression using

Origin 8.5[®] and the regression was assessed by ANOVA at the 95% level of significance.

3. Results and discussion

3.1 Point of zero charge (pH_{PZC}), pH and temperature effect

Figure 1 shows the variation of pH as a function of the initial pH for the three adsorbents: untreated, treated with H_3PO_4 and treated with NH_4Cl . The pH at the point of zero charge was approximately 5.0 for the natural rice husk, 2.5 for the treatment with H_3PO_4 and 5.0 for treatment with NH_4Cl . Below these values the solid presents a positive surface charge favoring the adsorption of anions. Then, it is expected better adsorption on the studied biomass at pH s below pH_{PZC} due to the anionic characteristic of 5G blue reactive dye in aqueous solution.

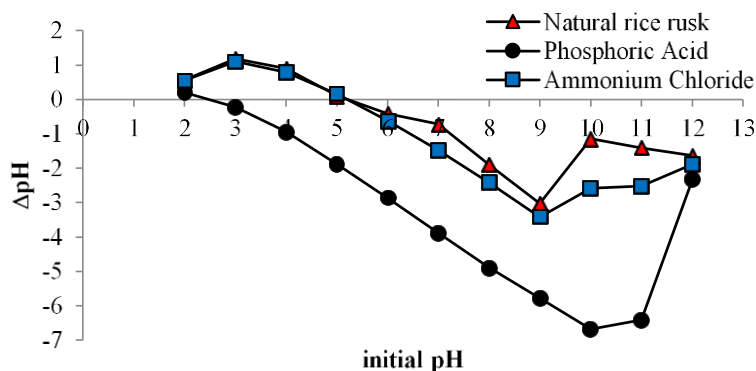


Figure 1. pH_{PZC} values for biosorbent rice husk natural and treated with H_3PO_4 and NH_4Cl .

Considering the value of the pH_{PZC} , the objective was to determine the pH range where the biosorbent adsorb more dye. Figure 2 presents the quantity of adsorbed dye (per adsorbent unit mass)

as a function of time, at different pH conditions and different adsorbents.

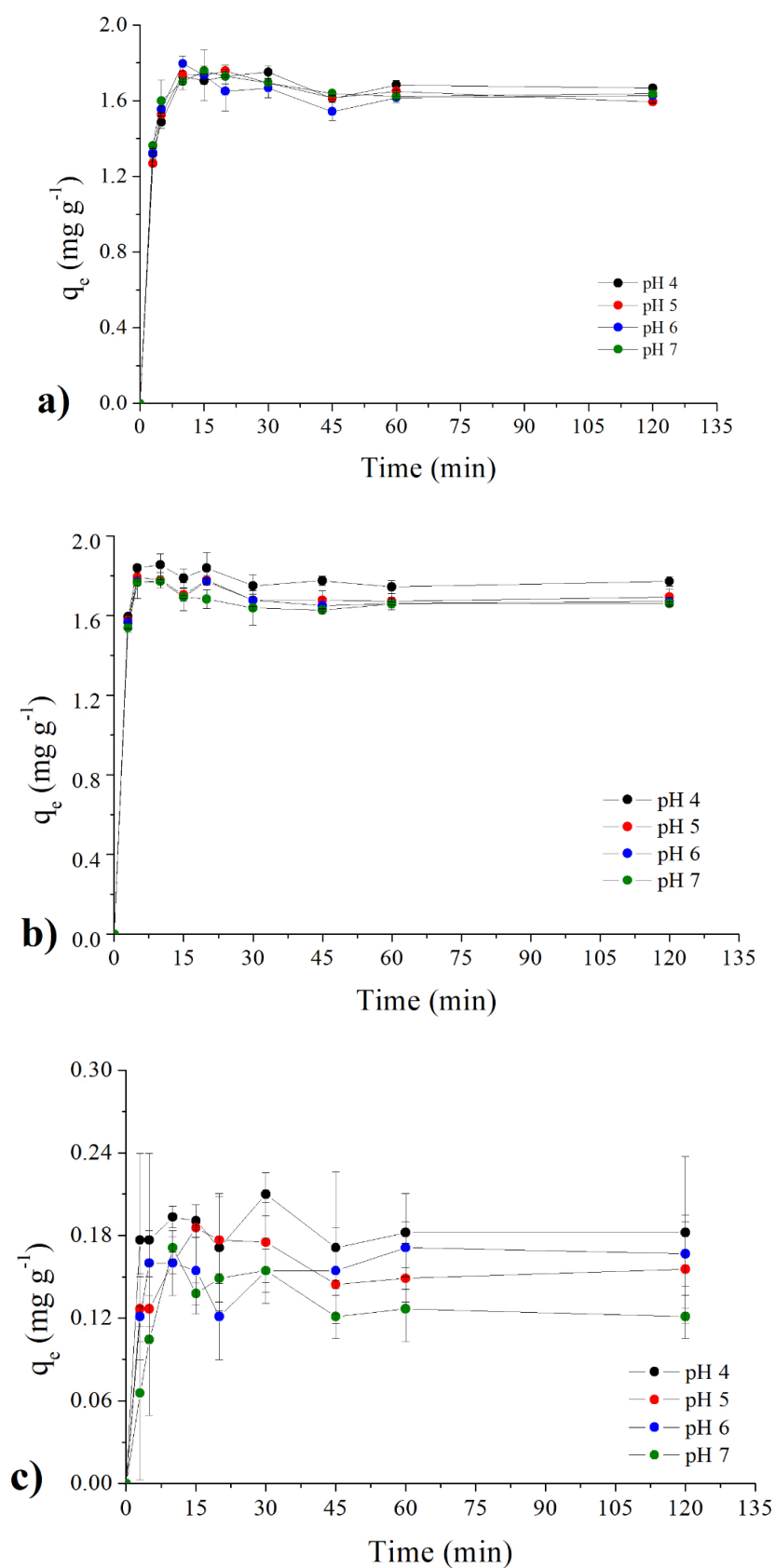


Figure 2. Influence of pH on biosorption (q_e) at 25 °C. a) natural rice rusk, b) H₃PO₄ and c) NH₄Cl.

It was observed that the biosorption of 5G Blue dye in solution by the rice hull is pH dependent. It was found that at pH 4 the natural biomass removed 81.3% of the dye, already for pH 5 it was 79.7%, for pH 6 it was 81.3% and pH 7 was 82.8%. In the pre-treatments the lower pHs were more efficient,

removing 88.6% of the dye by the biomass pretreated with phosphoric acid and 9.1% with ammonium chloride. Considering the time of 120 min the values of q_e were calculated for the studied pH values. These values are set forth in Table 1.

Table 1. Adsorption capacity of the study material (mg g^{-1}) at time 120 min for different pH values at 25 °C.

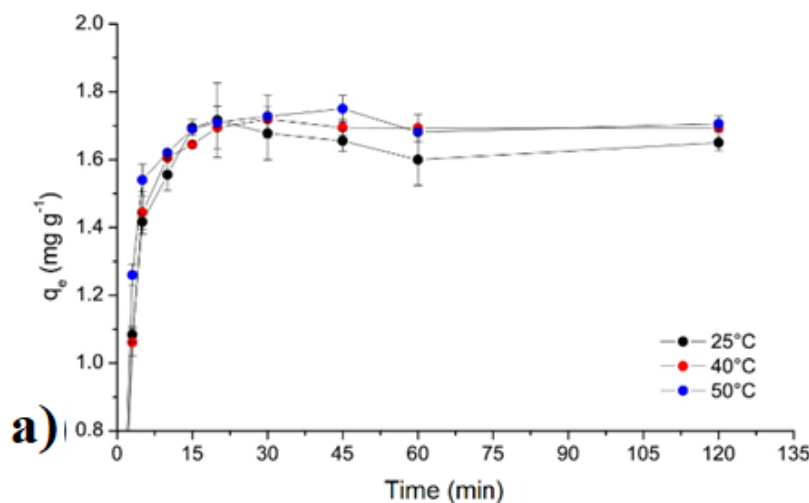
pH (A)	Treatments			t-test		
	Natural	H ₃ PO ₄ (B)	NH ₄ Cl (C)	AB	AB	BC
4	1.64(±0.03)	1.62(±0.01)	0.18(±0.02)	1.10	70.14	111.54
5	1.67(±0.04)	1.65(±0.04)	0.15(±0.01)	0.61	63.35	63.01
6	1.66(±0.01)	1.68(±0.02)	0.17(±0.01)	1.55	182.42	116.06
7	1.69(±0.03)	1.62(±0.01)	0.13(±0.03)	2.83	69.69	81.61

$t_{\text{critical}} (n=3; p=0.05) = 2.92$

For the comparison of the sorption capacity (q_e) between the treatments at each pH evaluated, the t-test was applied at a significance level of 95% (Table 1). Considering the degrees of freedom equal to 3, the critical value corresponds to $t_{(3; 0.05)} = 2.92$. All comparisons between the natural biosorbent and the H₃PO₄ (AB) treatment were considered statistically the same, since $t_{\text{critical}} > t_{\text{calculated}}$. However, for the biomass prepared with NH₄Cl, sorption capacity was different from the other treatments (AC and BC) because $t_{\text{critical}} < t_{\text{calculated}}$. Considering the lower values of q_e it can be considered that the application of NH₄Cl reduced the potential and sorption of the biomass studied and that the application of H₃PO₄ did not promote a statistically significant increase when compared to the natural biomass (Figure 2).

The pH can also affect the structural stability of the 5G blue reactive dye because, under an acidic condition, the dye molecule can be deprotonated within the solution, resulting in a polar molecule with a high negative charge density. Therefore, the electrostatic repulsion between the adsorbent site and the negatively charged dye ions was reduced at low pH. Consequently, positively charged functional groups could exert a strong electrostatic attraction on anionic dye molecules^{32, 33}.

An evaluation of the effect of the temperature considers a dye removal for each treatment at temperatures of 25, 40 and 50 °C. Figure 3 shows the experimental data of amount of dye adsorbed (q_e) versus time for each temperature studied at pH 4.



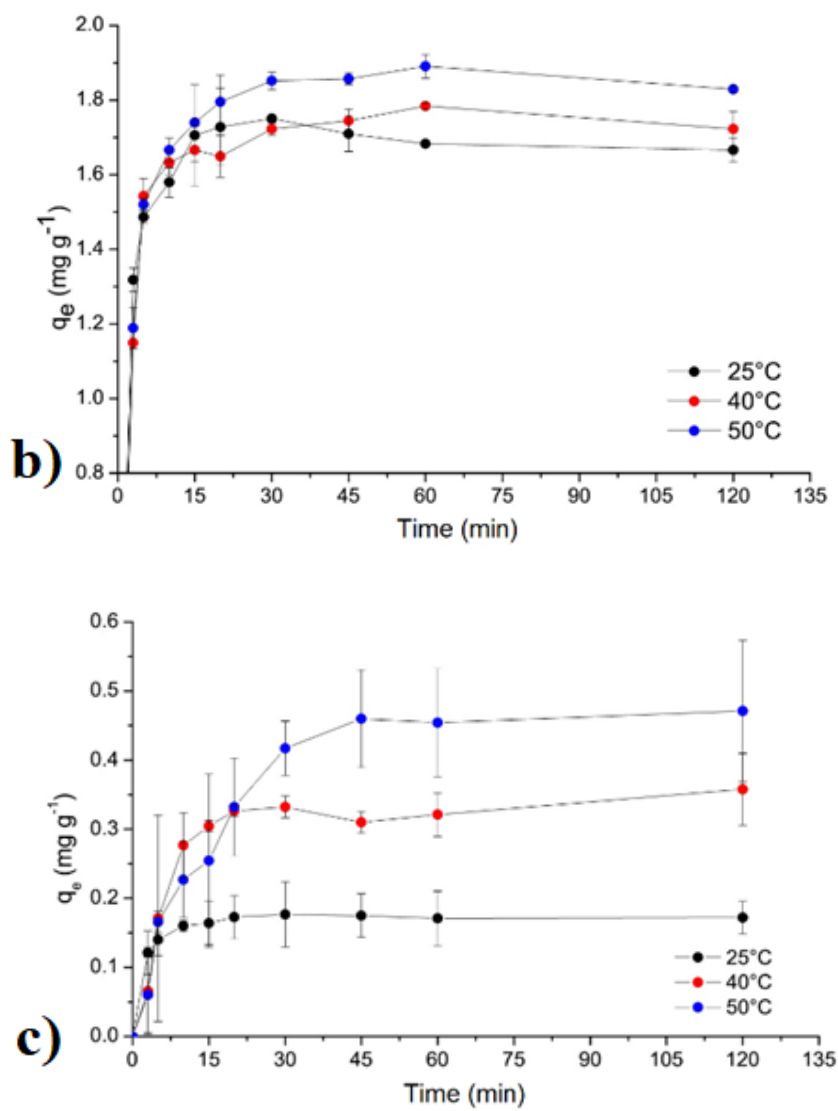


Figure 3. Influence of temperature on biosorption (q_e) at pH 4: a) natural rice rusk, b) H_3PO_4 and c) NH_4Cl .

The temperature significantly influences the kinetic energy of the molecules and interferes on the attraction and repulsion forces between the adsorbate and the adsorbent³³. In the range of temperature and conditions studied, an increase in the adsorbed amount was observed as the temperature increases, with 50 °C being the one that presented the best results. The biomass pretreated with H_3PO_4 at 50 °C showed the best dye removal, 91.5%. It was observed that an increase in temperature favorably influenced the ability of the 5G Blue dye to be removed by the rice husk biomass.

This behavior could be explained by factors such as an increased in mobility of the molecules present in the solution (increased kinetic energy

caused by the temperature rise), increased diffusion of adsorbate on the surface of the adsorbent, and dilation of the pores of the adsorbent³⁴.

3.2 Biosorption kinetic

Figure 4 shows the quantity of adsorbed dye per unit mass of adsorbent as a function of time, at pH 4 and 50 °C, for different pretreatments. The experimental data were adjusted to the models of pseudo-first order, pseudo-second order and intraparticle diffusion. The equilibrium time was about 20 min for *in natura* rice husk and about 35 min for both pretreated adsorbents.

Table 2 shows the fitted parameters and the determined coefficients for these experiments.

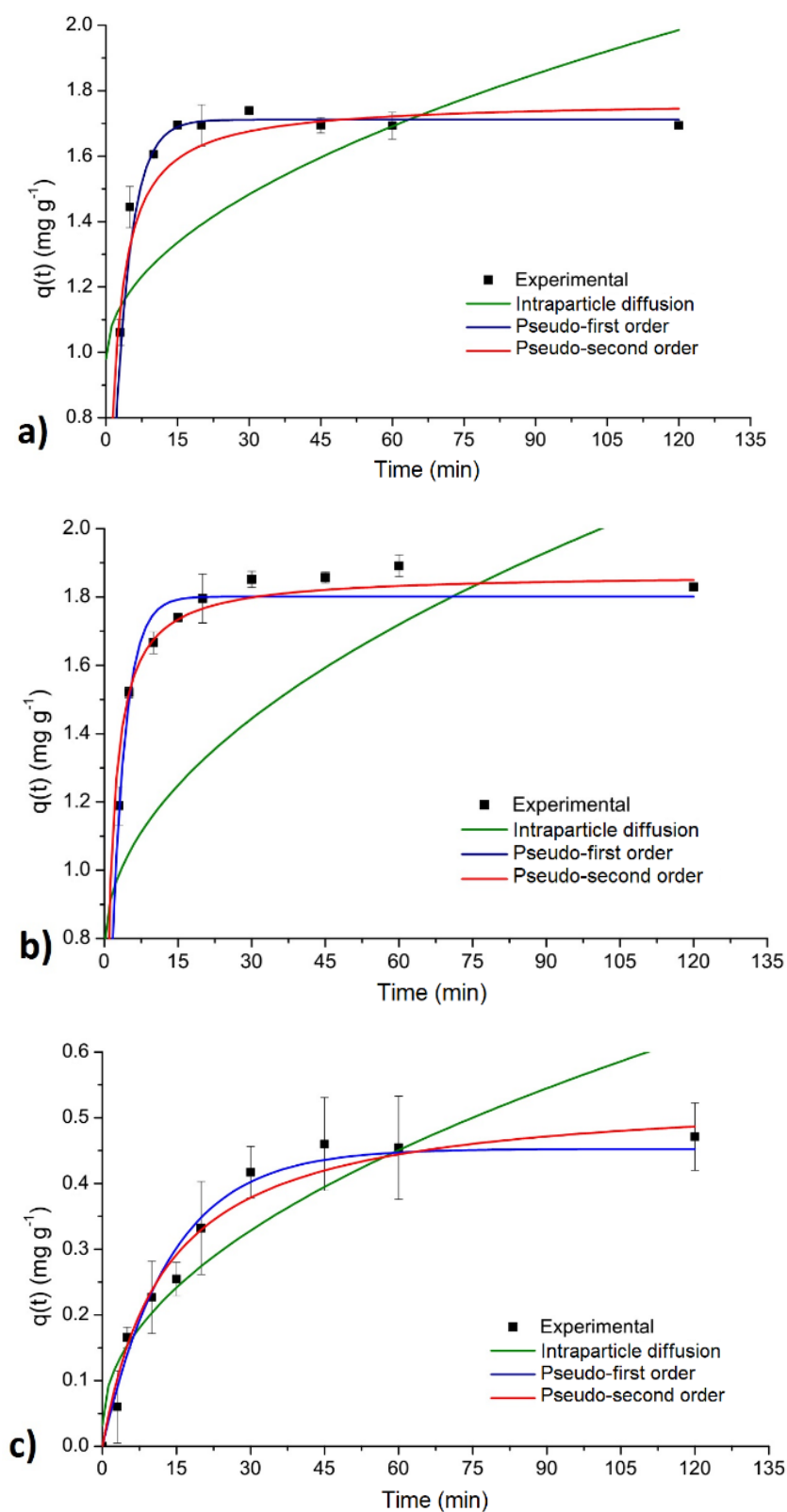


Figure 4. Experimental data and fit to intraparticle diffusion, pseudo-first and pseudo-second order models for the temperature of 50 °C and pH 4: a) natural rice rusk, b) H_3PO_4 and c) NH_4Cl .

Table 2. Parameters of the adsorption kinetic models of the 5G blue dye by the biomass with different pre-treatments for the conditions of pH 4 and temperature of 50 °C.

Treatment	Pseudo-first order			Pseudo-second order			Intraparticle diffusion		
	q_e^a	k_1^b	R^2	q_e^a	k_2^c	R^2	C	k_3^d	R^2
Natural	1.71	0.29	0.99	1.77	0.34	0.95	0.98	0.09	0.27
	(±0.01)	(±0.02)		(±0.01)	(±0.02)		(±0.28)	(±0.04)	
H ₃ PO ₄	1.80	0.35	0.99	1.87	0.47	0.99	0.78	0.12	0.44
	(±0.02)	(±0.03)		(±0.01)	(±0.05)		(±0.28)	(±0.04)	
NH ₄ Cl	0.45	0.07	0.96	0.54	0.15	0.97	0.03	0.05	0.88
	(±0.03)	(±0.01)		(±0.04)	(±0.03)		(±0.02)	(±0.01)	

^a q_e (mg g⁻¹); ^b k_1 (min⁻¹), ^c k_2 (g mg⁻¹ min⁻¹) and ^d k_3 (g mg⁻¹ min^{-1/2})

Determination coefficients (R^2) were obtained between 0.27 and 0.99, indicating that some models do not represent satisfactory experimental data (Table 1). The best fit was observed for the pseudo-first order model, being suitable for all pre-treatments. The pseudo-second order model was only suitable for the treatment with phosphoric acid. The intraparticle diffusion model presented a low correlation coefficient for all adsorption processes. Even though the correlation coefficient for the intraparticle diffusion model, using NH₄Cl-treated rice husk, was rather high (0.88), the C parameter presents a large standard deviation (66% of the mean value), which might impair its statistical significance.

The pseudo-first and pseudo-second order models presented similar performance in the fitting of the data. The removal values (q_e) predicted by the pseudo-first order model agrees with the equilibrium experimental data. This model considers that the occupation rate of the active sites is proportional to the number of active sites available in the adsorbent material³⁵.

The pseudo-first-order model also showed a better fitting in the biosorption of the 5G blue dye in a study using orange bagasse as a biosorbent prepared by dehydration at different temperatures. A k_1 in the value of 0.32 min⁻¹ at pH 2 and initial

concentration of 25 mg L⁻¹ has been reported³². The removal of reactive blue 5G (RB5G) dye in solution, 72 mg L⁻¹, using the drying biomass of banana pseudo stem was investigated at pH 1 and 30 °C. For the pseudo-first order model a k_1 of 0.84 mg g⁻¹ was obtained. This value is due to the higher concentration of dye applied in the test³⁶.

3.3 Equilibrium biosorption

Figure 5 shows the quantity of adsorbed dye per unit mass of adsorbent at equilibrium conditions as a function of the concentration of the supernatant solution at equilibrium conditions, at pH 4 and 50 °C, for *in natura* rice husk and H₃PO₄-treated rice husk. Equilibrium analyses with NH₄Cl-treated rice husk were not carried out due to the low removal of the dye. The observed result for this treatment should be at least similar to the *in natura* biomass. It is suggested that the ammonium ion was adsorbed by the material and thus limiting the biosorption capacity of the biomass, which would lead to low retention of the dye as verified.

The adjusted parameters for adsorption isotherms and ANOVA of regression are shown in Table 3.

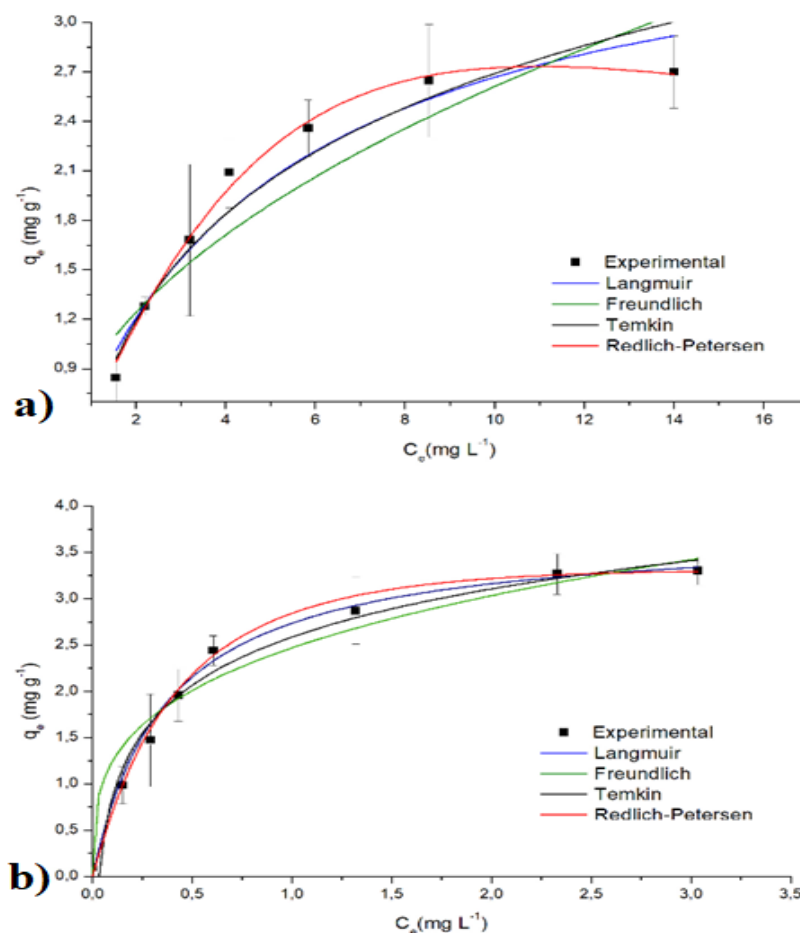


Figure 5. Experimental data and fit to Langmuir, Freundlich, Temkin and Redlich-Petersen isotherms at 50 °C and pH 4: a) natural and b) H₃PO₄.

Table 3. Isothermal parameters (Langmuir, Freundlich, Temkin and Redlich-Petersen) and ANOVA of regression for fitting the experimental data of biosorption of rice husk dye natural and pretreated with H₃PO₄.

Model		Treatment		ANOVA Regression			
		Natural	H ₃ PO ₄	Natural		H ₃ PO ₄	
				<i>F calc</i>	<i>p-value</i>	<i>F calc</i>	<i>p-value</i>
Langmuir	q_m	3.74 ± 0.09	3.8 ± 0.4				
	b	0.23 ± 0.04	2.7 ± 0.3	14.60	0.01	2.15	0.10
	R^2	0.98	0.95				
Freundlich	k_L	0.90 ± 0.09	2.5 ± 0.1				
	n	2.2 ± 0.3	3.4 ± 0.7	3.60	0.10	2.21	0.10
	R^2	0.86	0.89				
Temkin	B	0.93 ± 0.09	0.75 ± 0.06				
	k_T	1.8 ± 0.3	32 ± 9	3.20	0.10	2.16	0.20
	R^2	0.95	0.96				
Redlich-Petersen	k_R	0.64 ± 0.03	8.0 ± 0.8				
	a_R	0.03 ± 0.01	1.8 ± 0.3	60.00	0.00	11.17	0.04
	β	1.6 ± 0.1	1.13 ± 0.07				
	R^2	0.99	0.99				

$$F_{critical} (2.5; 0.05) = 5.8$$

Determination coefficients between 0.86 and 0.99 were observed, which means that some models do not represent the experimental data satisfactorily. The best fit was verified for the Redlich-Petersen model, being suitable for both the natural and the pre-treatment with H_3PO_4 . This model predicts a heterogeneous behavior on the surface of the adsorbent. The ANOVA at the 95% significance level for the evaluation of the fit of the models to the experimental data confirmed that the Redlich-Petersen model was more adequate, since it presented $F_{calc} > F_{critical}$ for the two treatments studied (60.0 and 11.17) as well as $p\text{-value} < 0.05$. It should also be noted that the Langmuir isotherm presented a favorable adjustment to the dye adsorption in the natural rice husk, with $R^2 = 0.98$ and $F_{calc} > F_{critical}$. When the constant β of Redlich-Petersen approaches 1 this equation takes the form of Langmuir. This model considers that the adsorbent has a limited number of positions on the surface. The molecules can be adsorbed to the point where all the surface sites are occupied, and adsorption will only occur in free sites, and when the equilibrium is reached no more interactions occur between the adsorbed molecules, nor between them and the medium³⁷. The maximum adsorbed value (q_m) of 3.81 mg g^{-1} predicted by the Langmuir model for the pretreated rice husk corroborates the experimental values.

The application of natural and citric acid treated rice hulls was evaluated in the Direct Red 23 dye biosorption. A q_m value was obtained for the Langmuir isotherm of 2.4 and 4.3 mg g^{-1} , respectively³⁸. These values were like those observed for the natural husk and treated with phosphoric acid (3.7 and 3.8 mg g^{-1}) presented in our study.

Removal of the reactive blue dye 4B using natural rice husk verified that Langmuir isotherm also better fitted to or the biosorption experimental data. Thus, it can be suggested that monolayer adsorption is occurred in this study³⁹. This also suggests that the intermolecular forces decrease rapidly with distance and consequently predicts the existence of monolayer coverage of the adsorbate at the outer surface of the adsorbent.

4. Conclusions

The best condition for the biosorption of the 5G blue reactive dye was the pretreatment with H_3PO_4 at pH 4 and $50 \text{ }^\circ\text{C}$, where there was removal of 91.5%. The process was favored in acidic media

and elevated temperatures. The kinetic models of pseudo-first and pseudo-second order satisfactorily described the experimental data with equilibrium time of approximately 20 min. The Langmuir and Redlich-Petersen isotherms satisfactorily described the experimental data indicating the maximum adsorbed value (q_m) of 3.81 mg g^{-1} . Thus, the results indicated that the rice husk showed a potential biosorbent for textile dye and could be used to control pollution.

5. Acknowledgments

The authors would like to thank UTFPR for material support.

6. References

- [1] Giovanella, R. F., Chiarello, L. M., Barcellos, I. O., Blosfeld, A. M., Remoção da cor de soluções de corantes reativos com cinza de casca de arroz, *Dynamis Revista Tecno-científica* 2 (15) (2009) 1-6.
- [2] Barakat, M. A., Adsorption and photodegradation of Procion yellow H-EXL dye in textile wastewater over TiO_2 suspension, *Journal of Hydro-environment Research*. 5 (2) (2011) 137-142. <https://doi.org/10.1016/j.jher.2010.03.002>.
- [3] Kimura, I. Y., Gonçalves Jr, A. C., Stolberg, J., Laranjeira, M. C. M., Fávere, V. T. de, Efeito do pH e do tempo de contato na adsorção de corantes reativos por microesferas de quitosana, *Polímeros* 9 (3) (1999) 51-57. <https://doi.org/10.1590/s0104-14281999000300010>.
- [4] Zouboulis, A. I., Loukidou, M. X., Matis, K. A., Biosorption of toxic metals from aqueous solutions by bacteria strains isolated from metal-polluted soils, *Process Biochemistry* 39 (8) (2004) 909-916. [https://doi.org/10.1016/s0032-9592\(03\)00200-0](https://doi.org/10.1016/s0032-9592(03)00200-0).
- [5] Castro, K. C. de, Cossolin, A. S., Reis, H. C. O. de, Morais, E. B. de, Biosorption of anionic textile dyes from aqueous solution by yeast slurry from brewery, *Brazilian Archives of Biology and Technology* 60 (2017) e17160101. <https://doi.org/10.1590/1678-4324-2017160101>.
- [6] Esposito, A., Pagnanelli, F., Lodi, A., Solisio, C., Vegliò, F., Biosorption of heavy metals by

- Sphaerotilus natans: an equilibrium study at different pH and biomass concentrations, *Hydrometallurgy* 60 (2) (2001) 129-141. [https://doi.org/10.1016/s0304-386x\(00\)00195-x](https://doi.org/10.1016/s0304-386x(00)00195-x).
- [7] Honorato, A. C., Machado, J. M., Celante, G., Borges, W. G. P., Dragunski, D. C., Caetano, J., Biossorção de azul de metileno utilizando resíduos agroindustriais, *Revista Brasileira de Engenharia Agrícola e Ambiental* 19 (7) (2015) 705-710. <https://doi.org/10.1590/1807-1929/agriambi.v19n7p705-710>.
- [8] Ozsoy, H., Kumbur, H., Adsorption of Cu(II) ions on cotton boll, *Journal of Hazardous Materials* 136 (3) (2006) 911-916. <https://doi.org/10.1016/j.jhazmat.2006.01.035>.
- [9] Gimbert, F., Morin-Crini, N., Renault, F., Badot, P.-M., Crini, G., Adsorption isotherm models for dye removal by cationized starch-based material in a single component system: Error analysis, *Journal of Hazardous Materials* 157 (1) (2008) 34-46. <https://doi.org/10.1016/j.jhazmat.2007.12.072>.
- [10] Liu, Y., Liu, Y.-J., Biosorption isotherms, kinetics and thermodynamics, *Separation and Purification Technology*, 61 (3) (2008) 229-242. <https://doi.org/10.1016/j.seppur.2007.10.002>.
- [11] Liu, Y., Liu, Y.-J., Reply to “Comments on “Biosorption isotherms, kinetics and thermodynamics” review”, *Separation and Purification Technology* 63 (2) (2008) 250-250. <https://doi.org/10.1016/j.seppur.2008.07.006>.
- [12] Nascimento, P., Marim, R., Carvalho, G., Mali, S., Nanocellulose Produced from Rice Hulls and its Effect on the Properties of Biodegradable Starch Films, *Materials Research* 19 (1) (2016) 167-174. <https://doi.org/10.1590/1980-5373-MR-2015-0423>.
- [13] Akhtar, M., Iqbal, S., Kausar, A., Bhangar, M. I., Shaheen, M. A., An economically viable method for the removal of selected divalent metal ions from aqueous solutions using activated rice husk, *Colloids and Surfaces B: Biointerfaces* 75 (2010) 149-155. <https://doi.org/10.1016/j.colsurfb.2009.08.025>.
- [14] Daffalla, S. B., Mukhtar, H., Shaharun, M. S., Characterization of adsorbent developed from rice husk: Effect of surface functional group on phenol adsorption, *Journal of Applied Sciences* 10 (2010) 1060-1067. <https://doi.org/10.3923/jas.2010.1060.1067>.
- [15] Naiya, T. K., Bhattacharya, A. K., Mandal, S., Das, S. K., The sorption of lead (II) ions on rice husk ash, *Journal of Hazardous Materials* 163 (2-3) (2009) 1254-1264. <https://doi.org/10.1016/j.jhazmat.2008.07.119>.
- [16] Ye, H., Zhu, Q., Du, D., Adsorptive removal of Cd (II) from aqueous solution using natural and modified rice husk, *Bioresource Technology* 101 (14) (2010) 5175-5179. <https://doi.org/10.1016/j.biortech.2010.02.027>.
- [17] El-Shafey, E. I., Removal of Zn(II) and Hg(II) from aqueous solution on a carbonaceous sorbent chemically prepared from rice husk, *Journal of Hazardous Materials* 175 (1-3) (2010) 319-327. <https://doi.org/10.1016/j.jhazmat.2009.10.006>.
- [18] Akhtar, M., Bhangar, M. I., Iqbal, S., Hasany, S. M., Sorption potential of rice husk for the removal of 2,4-dichlorophenol from aqueous solutions: Kinetic and thermodynamic investigations, *Journal of Hazardous Materials* 128 (1) (2006) 44-52. <https://doi.org/10.1016/j.jhazmat.2005.07.025>.
- [19] Goel, J., Kadirvelu, K., Rajagopal, C., Garg, V. K., Removal of lead (II) by adsorption using treated granular activated carbon: batch and column studies, *Journal of Hazardous Materials* 125 (1-3) (2005) 211-220. <https://doi.org/10.1016/j.jhazmat.2005.05.032>.
- [20] Vadivelan, V., Kumar, K. V., Equilibrium, kinetics, mechanism, and process design for the sorption of methylene blue onto rice husk, *Journal of Colloid and Interface Science* 286 (2005) 90-100. <https://doi.org/10.1016/j.jcis.2005.01.007>.
- [21] Sumanjit, N. P., Adsorption of dyes on rice husk ash, *Indian Journal of Chemistry Sec A* 40 (2001) 388-391.
- [22] Kosmulski, M., pH-dependent surface charging and points of zero charge II. Update, *Journal of Colloid and Interface Science* 275 (1) (2004) 214-224.

<https://doi.org/10.1016/j.jcis.2004.02.029>.

[23] Lagergren, S., Zur theorie der sogenannten adsorption gelöster stoffe, *Kungliga Svenska Vetenskapsakademiens Handlingar* 24 (4) (1898) 1-38.

[24] Ho, Y. S., McKay, G., Pseudo-second order model for sorption processes, *Process Biochemistry* 34 (5) (1999) 451-465. [https://doi.org/10.1016/s0032-9592\(98\)00112-5](https://doi.org/10.1016/s0032-9592(98)00112-5).

[25] Yang, X., Al-Duri, B., Kinetic modeling of liquid-phase adsorption of reactive dyes on activated carbon, *Journal of Colloid and Interface Science* 287 (1) (2005) 25-34. <https://doi.org/10.1016/j.jcis.2005.01.093>.

[26] Radhika, M., Palanivelu, K., Adsorptive removal of chlorophenols from aqueous solution by low cost adsorbent—Kinetics and isotherm analysis, *Journal of Hazardous Materials* 138 (1) (2006) 116-124. <https://doi.org/10.1016/j.jhazmat.2006.05.045>.

[27] Amuda, O. S., Giwa, A. A., Bello, I. A., Removal of heavy metal from industrial wastewater using modified activated coconut shell carbon, *Biochemical Engineering Journal* 36 (2) (2007) 174-181. <https://doi.org/10.1016/j.bej.2007.02.013>.

[28] Desta, M. B., Batch Sorption Experiments: Langmuir and Freundlich Isotherm Studies for the Adsorption of Textile Metal Ions onto Teff Straw (*Eragrostis tef*) Agricultural Waste, *Journal of Thermodynamics* 2013 (2013) 1-6. <https://doi.org/10.1155/2013/375830>.

[29] Ng, C., Losso, J. N., Marshall, W. E., Rao, R. M., Freundlich adsorption isotherms of agricultural by-product-based powdered activated carbons in a geosmin–water system, *Bioresource Technology* 85 (2) (2002) 131-135. [https://doi.org/10.1016/s0960-8524\(02\)00093-7](https://doi.org/10.1016/s0960-8524(02)00093-7).

[30] Gupta, V. K., Pathania, D., Singh, P., Kumar, A., Rathore, B. S., Adsorptional removal of methylene blue by guar gum–cerium (IV) tungstate hybrid cationic exchanger, *Carbohydrate Polymers* 101 (2014) 684-691. <https://doi.org/10.1016/j.carbpol.2013.09.092>.

[31] Hameed, B. H., Mahmoud, D. K., Ahmad, A. L., Equilibrium modeling and kinetic studies on the adsorption of basic dye by a low-cost adsorbent: Coconut (*Cocos nucifera*) bunch waste, *Journal of Hazardous Materials* 158 (1) (2008) 65-72. <https://doi.org/10.1016/j.jhazmat.2008.01.034>.

[32] Fiorentin, L. D., Trigueros, D. E., Módenes, A. N., Espinoza-Quiñones, F. R., Pereira, N. C., Barros, S. T., Santos, O. A., Biosorption of reactive blue 5G dye onto drying orange bagasse in batch system: Kinetic and equilibrium modeling, *Chemical Engineering Journal* 163 (1) (2010) 68-77. <https://doi.org/10.1016/j.cej.2010.07.043>.

[33] Fagundes-Klen, M. R., Cervelin, P. C., Veit, M. T., da Cunha Gonçalves, G., Bergamasco, R., da Silva, F. V., Adsorption Kinetics of Blue 5G Dye from Aqueous Solution on Dead Floating Aquatic Macrophyte: Effect of pH, Temperature, and Pretreatment, *Water, Air, & Soil Pollution* 223 (7) (2012) 4369-4381. <https://doi.org/10.1007/s11270-012-1201-x>.

[34] Saeed, A., Sharif, M., Iqbal, M., Application potential of grapefruit peel as dye sorbent: Kinetics, equilibrium and mechanism of crystal violet adsorption, *Journal of Hazardous Materials* 179 (1-3) (2010) 564-572. <https://doi.org/10.1016/j.jhazmat.2010.03.041>.

[35] Aksu, Z., Equilibrium and kinetic modelling of cadmium(II) biosorption by *C. vulgaris* in a batch system: effect of temperature, *Separation and Purification Technology* 21 (3) (2001) 285-294. [https://doi.org/10.1016/s1383-5866\(00\)00212-4](https://doi.org/10.1016/s1383-5866(00)00212-4).

[36] Módenes, A. N., Espinoza-Quiñones, F. R., Geraldi, C. A. Q., Manenti, D. R., Trigueros, D. E. G., Oliveira, A. P. da, Borba, C. E., Kroumov, A. D., Assessment of the banana pseudostem as a low-cost biosorbent for the removal of reactive blue 5G dye, *Environmental Technology* 36 (22) (2015) 2892-2902. <https://doi.org/10.1080/09593330.2015.1051591>.

[37] Sodr e, F. F., Lenzi, E., Costa, A. C. S. da, Utiliza o de modelos f sico-qu micos de adsor o no estudo do comportamento do cobre em solos argilosos, *Qu mica Nova* 24 (3) (2001) 324-330. <https://doi.org/10.1590/s0100-40422001000300008>.

[38] Abdelwahab, O., El-Nemr, A., El-Sikaily, A., Khaled, A., Use of rice husk for adsorption of direct dyes from aqueous solution: A case study of direct F. Scarlet, *Egyptian Journal of Aquatic Research* 31 (1) (2005) 1-11.

[39] Chowdhury, S., Saha, T. K., Removal of reactive blue 4 (RB4) onto puffed rice in aqueous solution, *International Journal of Advanced Research (IJAR)* 4 (3) (2016) 927-934.